BIOCHEMISTRY
including biophysical chemistry & molecular biology

Current Topic

pubs.acs.org/biochemistry

# [FeFe]-Hydrogenase Maturation

Eric M. Shepard, Florence Mus, Jeremiah N. Betz, Amanda S. Byer, Benjamin R. Duffus, John W. Peters, and Joan B. Broderick*

Department of Chemistry and Biochemistry, Montana State University, Bozeman, Montana 59717, United States

**ABSTRACT:** Hydrogenases are metalloenzymes that catalyze the reversible reduction of protons at unusual metal centers. This Current Topic discusses recent advances in elucidating the steps involved in the biosynthesis of the complex metal cluster at the [FeFe]-hydrogenase (HydA) active site, known as the H-cluster. The H-cluster is composed of a 2Fe subcluster that is anchored within the active site by a bridging cysteine thiolate to a [4Fe-4S] cubane. The 2Fe subcluster contains carbon monoxide, cyanide, and bridging dithiolate ligands. H-cluster biosynthesis is now understood to occur stepwise; standard iron−sulfur cluster assembly machinery builds the [4Fe-4S] cubane of the H-cluster, while three specific maturase enzymes known as HydE, HydF, and HydG assemble the 2Fe subcluster. HydE and HydG are both radical *S*-adenosylmethionine enzymes that interact with an iron−sulfur cluster binding GTPase scaffold, HydF, during the construction of the 2Fe subcluster moiety. In an unprecedented biochemical reaction, HydG cleaves tyrosine and decomposes the resulting dehydroglycine into carbon monoxide and cyanide ligands. The role of HydE in the biosynthetic pathway remains undefined, although it is hypothesized to be critical for the synthesis of the bridging dithiolate. HydF is the site where the complete 2Fe subcluster is formed and ultimately delivered to the immature hydrogenase protein in the final step of [FeFe]-hydrogenase maturation. This work addresses the roles of and interactions among HydE, HydF, HydG, and HydA in the formation of the mature [FeFe]-hydrogenase.

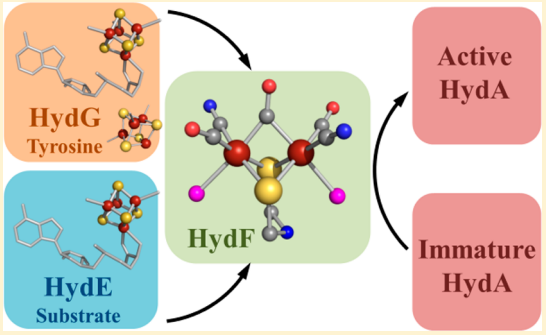


Hydrogenases are metalloenzymes that perform essential metabolic roles in many microbial communities by catalyzing the consumption and production of dihydrogen ($H_2$).[1,2] Their physiological role is either coupling hydrogen oxidation to anabolic processes or recycling reduced electron carriers during fermentation via the reduction of protons.[3] Although numerous enzymes catalyze reactions that use $H_2$ as a substrate or cosubstrate or generate $H_2$ as a product or coproduct, only two classes of hydrogenases catalyze the reversible interconversion of $H_2$ to protons and electrons; these enzyme classes have been termed the [NiFe]- and [FeFe]-hydrogenases on the basis of the metal composition of their respective active site metal centers.[4] The [NiFe]-hydrogenases are more commonly associated with $H_2$ oxidation under physiological conditions and contain a heterobimetallic active site with a Ni ion bridged to an Fe ion through two thiol groups supplied by cysteine side chains. Two additional cysteine thiols coordinate the nickel, and the iron is further coordinated by a carbon monoxide and two cyanide ligands.[5] The presence of these diatomic ligands to Fe was largely unanticipated; in fact, when the first structure of a hydrogenase enzyme was determined in 1995 by the Fontecilla-Camps group, electron density indicating nonprotein ligands bound to the Fe ion was tentatively assigned as arising from water molecules.[6] Only later when investigators examined the properties of carbon monoxide inhibition through infrared spectroscopy were the nonprotein ligands assigned carbon monoxide and cyanide.[7] Soon thereafter, the presence of carbon monoxide and cyanide ligands was more generally identified as being an intrinsic property of [NiFe]-hydrogenases.[8,9]

When the first structures of [FeFe]-hydrogenases were determined in the late 1990s, it was anticipated that the active site metal centers, like those of the [NiFe]-hydrogenases, possessed carbon monoxide and cyanide ligands, although there were ambiguities concerning the number and arrangement.[10,11] Two independent groups tentatively assigned five diatomic ligands to the active site and revealed a metal center consisting of a 2Fe subcluster, with one bridging and two terminal diatomics bound to each Fe ion. The assignment of the number of carbon monoxide and cyanide ligands was based on infrared (IR) studies.[8] Two terminal diatomic ligands were observed in the structures to be directly hydrogen bonded to protein groups and were thus assigned as the cyanide ligands.[11] The dithiolate ligand is also a unique feature of the [FeFe]-hydrogenases; however, its composition has eluded direct determination for more than a decade.[12−14]

In the initial structural work, there was a consensus that the ligand was a nonprotein dithiolate, i.e., a covalent linkage between two sulfur groups, but the structural work did not allow differentiation among C, N, and O at the bridgehead position.[10] The Fontecilla-Camps group originally assigned the ligand as propane dithiolate but later revised their assignment

**Received:** February 18, 2014
**Revised:** April 30, 2014
**Published:** May 30, 2014

   dx.doi.org/10.1021/bi500210x | *Biochemistry* 2014, 53, 4090−4104

to dithiomethylamine on the basis of mechanistic considerations that the bridgehead atom was poised to participate as a proton donor−acceptor group.[11,12] This was an insightful and attractive proposal; however, it lacked experimental support. A number of subsequent studies involving computational work examined different scenarios, including propanedithiol, dithiomethylamine, and dithiomethyl ether, with mixed results.[13,15,16] Essentially amine and ether functionalities at this position gave comparable agreement with the crystal structures, but the amine was more attractive as a potential proton donor and/or acceptor. Spectroscopic work did ultimately provide evidence of the presence of a nitrogen at this position.[17,18] Although the composition has still not been determined by direct analysis of the enzyme matured *in vivo*, reconstitution studies involving hydrogenase activation with 2Fe subcluster synthetic mimics have provided strong evidence that the ligand is dithiomethylamine,[19,20] removing ambiguities about the composition and architecture of the H-cluster (Figure 1).

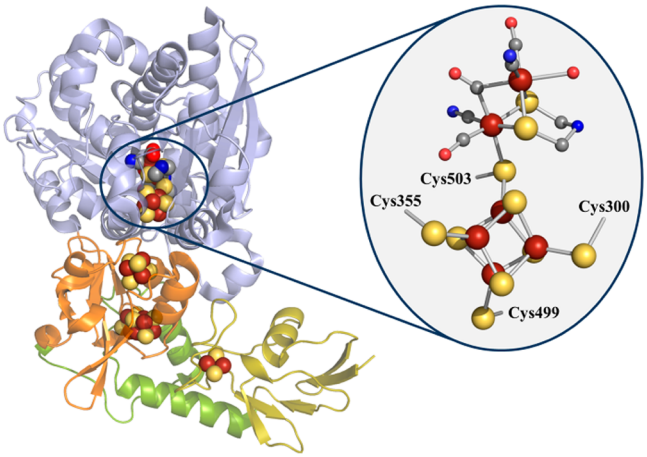


**Figure 1.** X-ray crystal structure of *Clostridium pasteurianum* I (CpI) [FeFe]-hydrogenase (PDB entry 3C8Y). CpI HydA (left) is composed of four domains. The catalytic domain containing the active site H-cluster (magnification, right) is colored light blue. Accessory iron−sulfur cluster domains are colored orange, green, and olive. Protein-bound iron−sulfur clusters are depicted as spheres. Color scheme: Fe, rust; S, yellow; C, gray; N, blue; O, red.

Although active site diatomic ligands are common features of the hydrogenases, [NiFe]- and [FeFe]-hydrogenases are not evolutionarily related.[21−24] [FeFe]-hydrogenases are found in several lower eukaryotes (algae and protists), and a wide range of bacteria but not cyanobacteria or archaea, whereas the [NiFe]-hydrogenases are present in cyanobacteria, archaea, and bacteria, but not in eukaryotes.[4,24] The protein most closely related to [FeFe]-hydrogenases is Narf or Nar1, a protein found only in eukaryotes that has a role in cytoplasmic iron−sulfur cluster biosynthesis and repair.[25] [NiFe]-hydrogenases are most closely related to subunits of Nuo or respiratory complex I.[26] Given the unique nature of the diatomic ligands, one might characterize hydrogenases as one of the most profound cases of convergent evolution.[27]

Further support for the convergent evolution of hydrogenases is the observation that [NiFe]- and [FeFe]-hydrogenase diatomic ligands are generated by completely different biochemical mechanisms. [NiFe]-hydrogenase maturation, including the synthesis of the unique diatomic ligands, involves a suite of maturase enzymes encoded by *hypABCDEF*.[21] The maturation scheme proposed by Watanabe et al. provides a working model of how the six maturase enzymes operate.[28] HypE and HypF interact stoichiometrically with a $K_D$ of 400 nM in their combined role of cyanide synthesis from carbamoyl phosphate and subsequent transfer to an Fe moiety likely bound to HypCD.[29−31] HypD serves as a scaffold for the synthesis of the Fe−$(CN)_2CO$ unit.[32] A recent spectroscopic investigation revealed that HypC bound $CO_2$, implicating this enzyme in the synthesis of the carbon monoxide ligand.[33] HypA (and its homologues) with HypB are required for insertion of the Ni ion into the immature hydrogenase protein *in vivo*, which is likely to follow the transfer of the decorated Fe atom to the immature hydrogenase.[28,34] [FeFe]-hydrogenase maturation requires the involvement of only three maturation proteins. Unlike the system employed for the production of the [NiFe]-hydrogenase active site, the critical steps during H-cluster biosynthesis involve radical *S*-adenosyl-L-methionine (SAM)-based chemical transformations. Radical SAM enzymes reductively cleave SAM into methionine and a 5′-deoxyadenosyl radical species (dAdo•) in a process coupled to abstraction of a H atom from substrate.[35] This Current Topic focuses on the experimental results in the [FeFe]-hydrogenase system and progress toward a pathway for the biological assembly of the H-cluster.

## IDENTIFICATION OF THE [FEFE]-HYDROGENASE MATURATION MACHINERY

Early efforts to heterologously overexpress HydA in *Escherichia coli* were plagued by the production of an inactive enzyme,[36,37] demonstrating the inability of *E. coli* to biosynthesize the H-cluster without specific maturases. It was not until 2004 that three hydrogenase accessory genes denoted *hydE*, *hydF*, and *hydG* were identified that when coexpressed with *hydA* could support the heterologous expression of active hydrogenase (Figure 2A).[38] It was further shown that hydrogenase activity was not observed in strains expressing HydA that lacked either *hydE*, *hydF*, or *hydG* (Figure 2C).[39] Importantly, the inactive enzyme obtained through expression of HydA alone in *E. coli* ($HydA^{\Delta EFG}$) could be activated by the *in vitro* addition of an *E. coli* lysate containing HydE, HydF, and HydG coexpressed together (Figure 2B); this result demonstrated that H-cluster assembly was achieved through the actions of these three enzymes with ubiquitous substrate(s) present in the cellular lysate.[22] Hydrogenase activity was, however, not observed when lysate mixtures of the maturases expressed either singly or in varying combinations in independent cell lines were added to $HydA^{\Delta EFG}$.[22] Because the substrates for H-cluster ligand synthesis were unknown at this time and not added to the *in vitro* activation assay, the results were interpreted to indicate that a preformed cluster intermediate was synthesized by HydE, HydF, and HydG that could be transferred to HydA to effect activation.

Sequence annotation of the maturase enzymes identified HydE and HydG as belonging to the radical SAM superfamily of enzymes because of the canonical $CX_3CX_2C$ motif.[38−41] HydF, on the other hand, contains the N-terminal Walker A P-loop and Walker B $Mg^{2+}$ binding motifs associated with small Ras GTPases, as well as several putative C-terminal metal binding residues that indicate this enzyme binds iron−sulfur (FeS) clusters. The work of King et al. demonstrated that the $CX_3CX_2C$ motifs in HydE and HydG, and the FeS cluster and GTP binding regions of HydF, were all essential to [FeFe]-hydrogenase activation.[39] These findings led us to develop a


dx.doi.org/10.1021/bi500210x | *Biochemistry* 2014, 53, 4090−4104

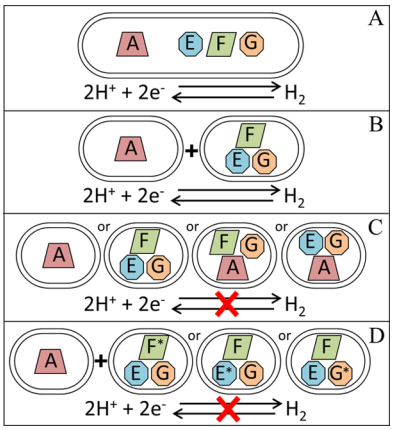


**Figure 2.** Whole cell extract hydrogenase activation results for the *Clostridium acetobutylicum* maturases. (A) HydAEFG coexpression yields hydrogenase activity. (B) HydA expressed singly can be activated by coexpressed HydEFG. (C) No hydrogenase activity is obtained in the absence of either one maturase enzyme or all maturase enzymes. (D) HydE, HydF, or HydG variant proteins coexpressed with their wild-type partners cannot activate HydA.[39] The asterisk denotes variant proteins. In the case of HydF, the variants contain point mutations of residues in either the P-loop or FeS cluster binding motifs. For HydE and HydG, point mutations of the conserved $CX_3CX_2C$ residues, as well as the residues of the accessory C-terminal cluster motif in HydG, all proved to be deleterious to hydrogenase maturation.

hypothetical pathway for H-cluster assembly in which HydE and HydG synthesized the 2Fe subcluster on the scaffold HydF through the modification of a [2Fe-2S] cluster; alkylation of the sulfide groups was proposed to occur in a first step followed by the decomposition of an amino acid radical into CO and $CN^-$.[42] Moreover, we hypothesized that HydE, HydF, and HydG were solely directed at 2Fe subcluster biosynthesis, whereas standard FeS cluster assembly machinery (either the ISC or SUF systems) manufactured the [4Fe-4S] cubane of the H-cluster.[42]

## HYDA EXPRESSED WITHOUT MATURASES BINDS THE [4FE-4S] CUBANE OF THE H-CLUSTER

[FeFe]-hydrogenase enzymes all contain a common active site domain that houses the H-cluster (Figure 1) but vary in the number and arrangement of the accessory FeS clusters involved in the transfer of an electron to and from the active site during catalysis.[2] [FeFe]-hydrogenase from the green algae *Chlamydomonas reinhardtii* (*Cr*) has become the focus of many biochemical and spectroscopic studies because it lacks accessory FeS clusters, thereby simplifying characterization.[43−50] Analysis of *Cr* $HydA^{\Delta EFG}$ overexpressed in *E. coli* revealed UV−visible, EPR, and Mössbauer spectroscopic features typical of $[4Fe\text{-}4S]^{2+/+}$ clusters.[47] While neither the as-purified states nor the metal free states of the *Cr* $HydA^{\Delta EFG}$ enzyme were active, hydrogenase activity was observed when either the as-purified or chemically reconstituted form was incubated with an *E. coli* cell extract containing HydE, HydF, and HydG (Figure 2B). $HydA^{\Delta EFG}$ in which the [4Fe-4S] cluster had been removed by iron chelation could not be activated in the presence of the HydE/HydF/HydG extract unless the [4Fe-4S] cluster was first in place. These results demonstrated the requirement for preassembly of the [4Fe-4S] cubane component of the H-cluster, which is presumably synthesized by either the ISC or SUF systems *in vivo*, prior to activation by the hydrogenase maturation enzymes.[47] Further support for this assembly mechanism has come from NRVS and EPR studies with *Clostridium pasteurianum* I (CpI) HydA.[51] Kuchenreuther and co-workers have reported that when $^{56}$Fe-loaded $HydA^{\Delta EFG}$ is activated *in vitro* with $^{57}$Fe-labeled HydE, HydF, and HydG lysates enriched with exogenous $^{57}$Fe, the $^{57}$Fe isotope became associated with the 2Fe subcluster and not the [4Fe-4S] cubane of the H-cluster.[51] Together, these results clearly demonstrate that the hydrogenase maturation machinery is directed at the synthesis of only the 2Fe subcluster and not the entire 6Fe H-cluster.

Comparison of the X-ray crystal structure of the active site domains of *Cr* $HydA^{\Delta EFG}$ (PDB entry 3LX4) (Figure 3A) with that of CpI HydA provided insight into the mechanism for cluster insertion and the maturation process.[50] $HydA^{\Delta EFG}$ possesses an electropositive channel possibly providing favorable electrostatic interactions with the presumably negatively charged 2Fe subcluster fragment. Furthermore, as this channel is lined with water molecules leading to the active site, perhaps the 2Fe subcluster insertion reaction is entropically driven.[2] In CpI HydA, the channel is occupied by two loop regions conserved across HydA proteins that presumably rearrange upon 2Fe subcluster insertion enclosing the active site, and yielding HydA activation (Figure 3B).[2,50,52] The

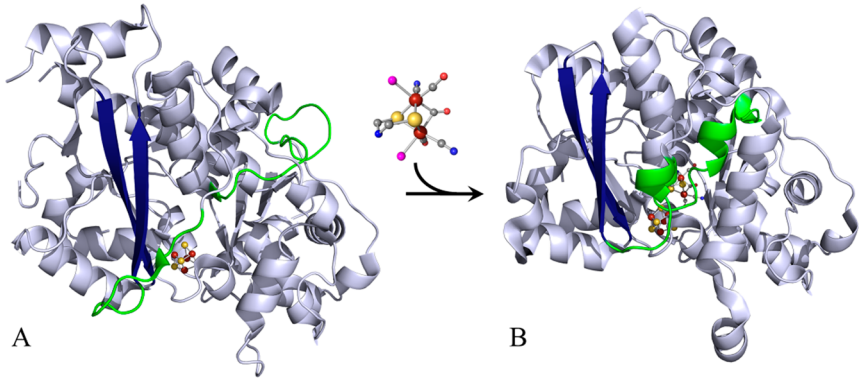


**Figure 3.** Insertion of the 2Fe subcluster into HydA. (A) The immature *Cr* HydA (PDB entry 3LX4) contains the [4Fe-4S] cubane of the H-cluster. (B) The holo CpI HydA (PDB entry 3C8Y) includes the active site H-cluster. The accessory FeS cluster domains have been omitted for the sake of clarity. The two $\beta$-strands in both structures are colored deep blue to emphasize structural similarities. The loop region that moves during 2Fe subcluster insertion is colored green. Color scheme: Fe, rust; S, yellow; C, gray; N, blue; O, red; undefined, magenta (see the legend of Figure 5).


dx.doi.org/10.1021/bi500210x | *Biochemistry* 2014, 53, 4090−4104

protein surface of HydA at the channel opening contains residues Arg315, Glu320, Asp325, Lys328, Lys433, Gln437, and Lys449, which may facilitate binding interactions with HydF during the cluster insertion process.[50]

## HYDF AS A SCAFFOLD OR CARRIER FOR THE 2FE SUBCLUSTER

$HydA^{\Delta EFG}$ activation experiments demonstrate that hydrogenase activity is observed when the enzyme is mixed with an extract of *E. coli* expressing HydE, HydF, and HydG in concert (Figure 2B).[22,47] Hydrogen evolution assays performed with $HydA^{\Delta EFG}$ and *Clostridium acetobutylicum* (*Ca*) HydE, HydF, or HydG purified proteins from an extract of *E. coli* expressing all three maturases ($HydE^{FG}$, $HydF^{EG}$, and $HydG^{EF}$) showed that only $HydF^{EG}$ can support activation.[53] Importantly, activation occurs without the addition of any exogenous small molecules or potential precursors of nonprotein ligands, suggesting $HydF^{EG}$ harbors an H-cluster 2Fe subcluster precursor that effects maturation of [FeFe]-hydrogenase, potentially in a manner analogous to the scaffold-directed biosynthesis of the nitrogenase FeMo cofactor.[54] The results supported a model in which HydF acts as either a scaffold or carrier protein for the H-cluster precursor moiety that is synthesized through the actions of HydE and HydG.

**HydF Iron–Sulfur Cluster States.** Chemically reconstituted and dithionite-reduced *Thermotoga maritima* (*Tm*) HydF expressed singly ($HydF^{\Delta EG}$) exhibits an axial EPR signal with *g* values of 2.045 and 1.904, indicative of the presence of FeS clusters.[55] Several additional studies have now probed FeS cluster binding in heterologously and homologously expressed HydF from *Ca*, *Thermotoga neopolitana* (*Tn*), and *Shewanella oneidensis* (*So*).[56−61] In our work, UV−visible spectra of the anaerobically purified, heterologously expressed *Ca* $HydF^{EG}$ and $HydF^{\Delta EG}$ proteins exhibit clear differences in the ligand to metal charge transfer features of bound FeS clusters; the greater absorbance in the ∼575 nm region of $HydF^{\Delta EG}$ samples was proposed to be indicative of $[2Fe\text{-}2S]^{2+}$ clusters.[53] Low-temperature EPR studies of as-purified *Ca* $HydF^{EG}$ and $HydF^{\Delta EG}$ samples revealed nearly isotropic signals centered at a *g* value of 2.00 typical of $[3Fe\text{-}4S]^{+}$ clusters. Following photoreduction with 5-deazariboflavin, the $[3Fe\text{-}4S]^{+}$ cluster signals in both $HydF^{EG}$ and $HydF^{\Delta EG}$ were replaced by identical axial signals that displayed fast temperature relaxation properties assigned to $[4Fe\text{-}4S]^{+}$ clusters with *g* values of 2.05, 1.89, and 1.86.[56,59] Importantly, a more prominent overlapping axial signal with *g* values of 2.01, 2.00, and 1.96 was present in reduced $HydF^{\Delta EG}$ that was found to have much slower temperature relaxation properties; these characteristics together with the observations from the UV−visible spectroscopy support the assignment of this signal as originating from a $[2Fe\text{-}2S]^{+}$ cluster.[56,59] Similar spectra have now also been reported by Berto et al. and Albertini et al. for dithionite-reduced samples of *Tn* and *Ca* $HydF^{\Delta EG}$; although the authors suggested that the overlapping $g \approx 2.0$ centered signal arose from a radical in the proximity of the $[4Fe\text{-}4S]^{+}$ cluster, the source of such a radical is neither examined nor discussed in this work.[61,62]

In a third independent study, variable-temperature EPR data collected with dithionite-reduced *So* $HydF^{\Delta EG}$ exhibited only a strong axial signal attributed to $[4Fe\text{-}4S]^{+}$ clusters, with no evidence of an overlapping $g \approx 2$ centered signal;[60] these authors suggested that our photoreduced samples may have had remnant $[3Fe\text{-}4S]^{+}$ cluster species or that the signal we have assigned as originating from a $[2Fe\text{-}2S]^{+}$ cluster could be the result of a protein-associated radical.[60] We find the former suggestion to be unlikely as $[3Fe\text{-}4S]^{+}$ clusters are typically rapidly reduced even with much milder reductants; further, our preparations of *Ca* HydF continue to show a $g \approx 2.0$ signal typical of $[3Fe\text{-}4S]^{+}$ clusters in their as-purified state, with photoreduction resulting in the two overlapping axial signals with the distinct *g* values that we initially reported.[56,59] Our results are also in line with the results observed for variant and wild-type forms of *Ca* and *Tn* HydF for which a similar overlapping $g \approx 2.0$ signal has been reported.[61,62] We have proposed that the [2Fe-2S] site could be a precursor for the 2Fe subcluster that is modified by the addition of nonprotein ligands catalyzed by HydE and HydG.[54,56]

FTIR analysis of as-purified *Ca* $HydF^{EG}$ revealed Fe−CO (1940 and 1881 $cm^{-1}$) and $Fe-CN^{-}$ (2046 and 2027 $cm^{-1}$) vibrations (Figure 4), whereas characterization of $HydF^{\Delta EG}$ demonstrated that no iron-bound diatomic species were present.[56] Czech et al. performed similar spectroscopic characterization of *Ca* $HydF^{EG}$ that was homologously overexpressed, and their FTIR spectra showed multiple vibrational features assigned to $Fe-CN^{-}$, Fe−CO, and Fe−CO−Fe species (Figure 4).[57] Moreover, an additional high-field component in the EPR spectrum coupled to the slower relaxation of this signal was attributed by the authors to arise from "a cluster which contains three or less irons".[57] Comparative XAS studies of active *Cr* HydA1 and *Ca* HydF enzymes and their inactive counterparts ($HydA^{\Delta EFG}$ and $HydF^{\Delta EG}$, respectively) did provide evidence of both [4Fe-4S] and 2Fe species associated with $HydF^{\Delta EG}$ and also demonstrated that the *n*Fe−*n*S−*n*O/N species present on $HydF^{EG}$ were similar to those measured for the H-cluster in active HydA.[58] Together, these data provided strong support for a 2Fe subcluster H-cluster precursor bound by HydF that

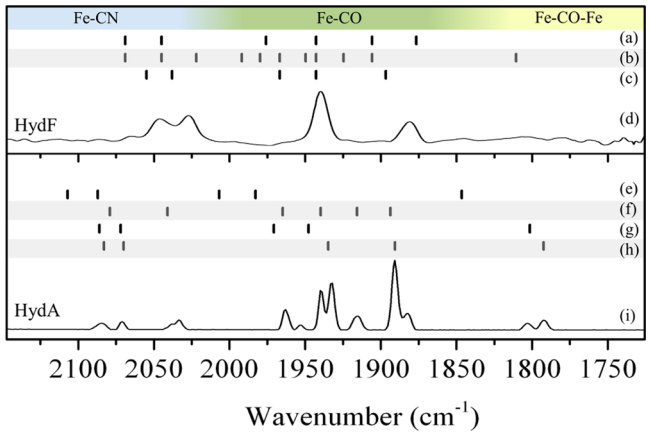


**Figure 4.** Summary of published HydF and HydA FTIR data. The top panel illustrates FTIR bands reported for the iron−diatomic species observed in HydF, while the bottom panel depicts the FTIR bands for the H-cluster in HydA. The HydF panel includes data from (a) nonreduced *Ca* $HydF^{EG}$,[57] (b) reduced *Ca* $HydF^{EG}$,[57] and (c) *Tm* HydF hybrid protein made with a biomimetic 2Fe subcluster mimic containing the dithiomethylamine bridge[19] and (d) a spectrum of as-isolated *Ca* $HydF^{EG}$.[56] Vibrational bands for the H-cluster include data for (e) as-isolated *Dd*,[12] (f) reduced *Dd*,[12] (g) as-isolated *Cp*,[63] and (h) reduced *Cr*HydA1[48] and (i) a spectrum of *Cr*HydA1 reduced with exogenous $H_2$.[65] For a more thorough summary of FTIR bands associated with the H-cluster, see ref 66.


dx.doi.org/10.1021/bi500210x | *Biochemistry* 2014, 53, 4090−4104

resembles the 2Fe subcluster of the [FeFe]-hydrogenase (Figures 5 and 6). Although the FTIR vibrational modes

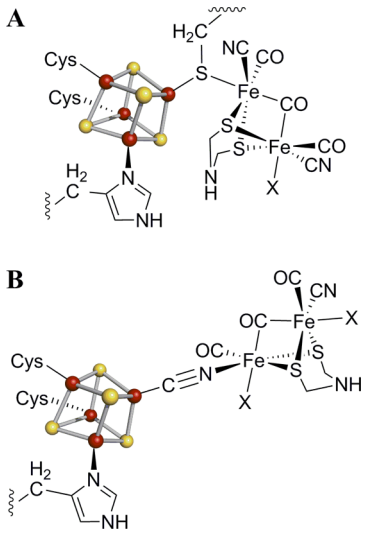


**Figure 5.** Hypothetical coordination environments for the 2Fe subcluster bound to *C. acetobutylicum* HydF. Cysteine and histidine ligands are presumed to be derived from both monomeric subunits, as FeS clusters are likely bound at the dimeric interface. Evidence of coordination of the histidine nitrogen to the [4Fe-4S] cubane has been provided by spectroscopic studies for *Ca* HydF (see the text). HydF proteins from *Tm* and *Tn* appear to have an exchangeable coordination site to the [4Fe-4S] cubane, and accordingly, the histidine in the representations given above could be replaced by an X for unknown. (A) Bridging cysteine thiolate coordination as proposed in ref 58. (B) Shared cyanide coordination as has been observed for 2Fe subcluster mimics bound to HydF.[19] The mechanism of cluster transfer for panel B would require cyanide linkage isomerism. Cluster transfer involving the cysteine thiolate coordination in panel A would appear to involve a ligand exchange mechanism. The [4Fe-4S] cluster in both panels is depicted as a ball and stick diagram with iron ions colored rust and sulfide ions colored yellow. We have attempted to preserve the octahedral environment of the Fe ions in these species and accordingly use the X in panels A and B to represent unknown coordination of the 2Fe subcluster when bound to HydF, possibly being either protein- or solvent-derived in nature. In Figures 3, 6, and 8, we utilize magenta spheres to illustrate this concept.

observed for $HydF^{EG}$ preparations were slightly different from those reported for the H-cluster itself (Figure 4),[8,63−66] given the sensitivity of these modes to the electron richness of the metal and the polarity of the ligand environment, the small differences in the Fe−$CN^-$ and Fe−CO vibrational modes likely reflect variations in the 2Fe subcluster environment between HydA and HydF.

It was recently demonstrated that 2Fe subcluster synthetic analogues each containing four terminally bound CO ligands, two terminally bound $CN^-$ ligands, and either propanedithiolate, dithiomethylamine, or dithiomethyl ether as a bridging dithiolate ligand can be loaded into chemically reconstituted *Tm* HydF and then delivered to $HydA^{\Delta EFG}$; in the case of the dithiomethylamine-containing species, the result is maximally active [FeFe]-hydrogenase.[19] Spectroscopic analysis indicated that when these cluster mimics are bound to HydF, one of the cyanide ligands forms a bridge to the [4Fe-4S] cubane (Figure 5B).[19] Further studies have now demonstrated that *in vitro* activation of $HydA^{\Delta EFG}$ with the 2Fe subcluster mimics can occur in a manner that is completely

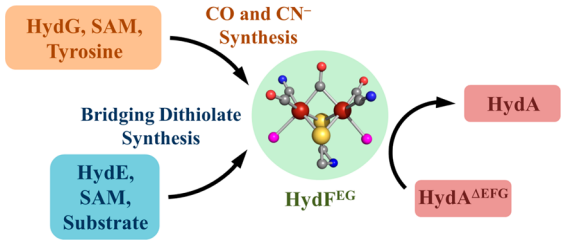


**Figure 6.** Hypothetical maturation scheme for H-cluster biosynthesis. HydG utilizes SAM and tyrosine to catalyze the formation of CO and $CN^-$ species. HydE uses SAM and an unidentified substrate to presumably synthesize the bridging dithiolate moiety. HydF likely acts as a scaffold protein during biosynthesis, and following interaction with HydE and HydG, HydF transiently binds a 2Fe subcluster precursor that resembles that of the H-cluster (see Figure 5; the [4Fe-4S] cubane bound by HydF is not shown for the sake of clarity). [FeFe]-hydrogenase maturation is then accomplished through the transfer of the 2Fe subcluster from HydF to $HydA^{\Delta EFG}$. Three possible scenarios for the delivery of CO and $CN^-$ from HydG to HydF include (a) delivery of diatomics as free ligands to an alkylated [2Fe] cluster intermediate bound to HydF, (b) HydG-derived Fe−(CO)CN species displacing a placeholder [2Fe-2S] cluster bound to HydF, or (c) insertion of HydG-derived Fe−(CO)CN group(s) into a vacant cavity in the scaffold protein. In cases b and c, it is plausible that two Fe−(CO)CN groups are joined together on HydF via the delivery of the dithiomethylamine ligand. Color scheme: Fe, rust; S, yellow; C, gray; N, blue; O, red; undefined, magenta (see the legend of Figure 5).

independent of HydF.[20] Following the unimpeded integration of the mimic into the hydrogenase active site, free CO can be detected in assays, indicating that upon incorporation into hydrogenase the fourth CO ligand of the analogue is released into solution. While it has been proposed that this fourth CO ligand could be present in HydF during *in vivo* maturation, no experimental evidence has been reported to support this hypothesis.[20,66]

The production of a 2Fe subcluster intermediate with four CO and two $CN^-$ ligands on HydF would require four distinct HydG turnover events (see Radical SAM Chemistry and Diatomic Ligand Synthesis). Although the results of the mimetic-based activation involving clusters with this diatomic ligand stoichiometry are intriguing, it might be premature to conclude that a cluster with such a composition is an intermediate in H-cluster biosynthesis.[66] The biological production of such an intermediate would be associated with the release of diatomic ligands (both CO and $CN^-$) in the cell, and while this is possible, it does seem unlikely. It has been observed that purified $HydF^{EG}$ exhibits low levels of hydrogenase activity, with <1% of the activity of the CpI HydA enzyme,[67] and it was reported that the HydF containing the dithiomethylamine-ligated 2Fe subcluster analogue did not produce any measurable hydrogenase activity,[19] suggesting that possible differences exist.

Additional work involving $HydA^{\Delta EFG}$ activation experiments involving a cell free protein synthesis system reported that only reaction mixtures containing HydE and HydG or HydF and HydG resulted in low levels of hydrogenase activity, suggesting HydG was the only maturase whose presence was absolutely required. Moreover, they reported 100% hydrogenase activation could be obtained when clarified cell lysate mixtures were used that lacked HydF, although their results also showed that expression of HydA in a background of only HydE and HydG or HydF and HydG did not support the production of active HydA.[60] The latter results are in line with previous observations

that showed that all three maturases are required for heterologous expression of active hydrogenase in *E. coli*, and that even site specific amino acid substitutions of the maturases can prevent the synthesis of active [FeFe]-hydrogenase (Figure 2).[22,39,53] Clearly, the differences between the results from the *in vitro* cell free synthesis system suggesting a nonessential role for HydF and those from *in vivo* studies supporting an essential role for HydF need to be resolved.

**HydF Structure.** Purified HydF proteins from both *Ca* and *Tn* heterologously overexpressed in *E. coli* exist as a mixture of dimers and tetramers, and both forms appear to coordinate FeS clusters given their visible absorbance spectra.[56,59,68] Structural studies suggested that the purified dimer species is converted to a metal free tetramer form during the crystallization process, stabilized by an interdimer disulfide bond (Figure 7).[68] Each subunit can be divided into GTPase, FeS cluster binding, and dimerization domains.[68]

Although the metal free HydF structure does not provide any direct insights into FeS composition or ligation, the putative cluster binding residues in the $CXHX_{46-53}HCXXC$ motif from two subunits are observed to approach one another at the dimer interface in the tetrameric structure (Figure 7). This localization of two sets of putative cluster ligands could explain how the limited number of Cys and His ligands could coordinate multiple clusters and/or cluster types during 2Fe subcluster biosynthesis. Ligands are also located in loop regions in a cleft that presumably would allow for substantial degrees of freedom for cluster rearrangement. The dimer observed in solution is likely to exist with both the GTP binding environment and FeS cluster(s) site exposed to solvent, potentially providing a mechanism for facilitating the transfer of the 2Fe subcluster to $HydA^{\Delta EFG}$. We propose that dimeric HydF is the form involved in activation of HydA (Figure 8).

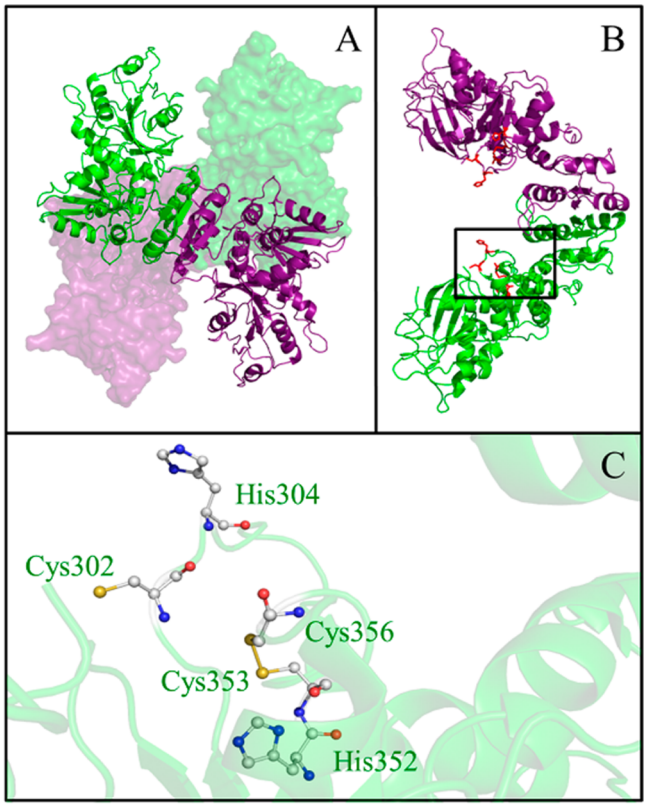


**Figure 7.** HydF structure. (A) Tetramer. The tetramer is a dimer of homodimers; here one dimer is a cartoon representation (front), and one dimer is a surface representation (back). Within the dimer, one monomer is green and the other purple. (B) Dimer. This image demonstrates the alignment of the FeS domains in the subunits of the dimer and the exposure of the GTPase domains at the far ends of the dimer. One monomer is colored green and one purple, and the cluster binding residues are colored red. (C) This expanded view of the box within panel B illustrates the putative residues associated with cluster binding. The residue numbers are for *Tn* HydF (PDB entry 3QQ5). Color scheme: S, yellow; C, gray; N, blue; O, red.

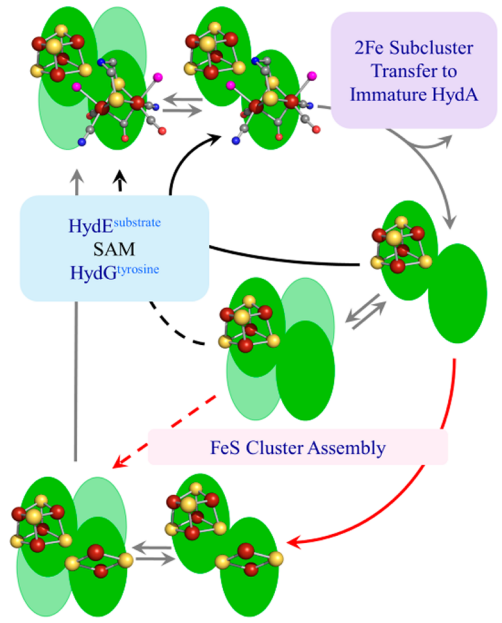


**Figure 8.** Hypothetical scheme detailing the proposed roles of the different oligomeric forms of HydF in H-cluster biosynthesis. Four pathways are depicted in this representation of putative cluster assembly on HydF. Two pathways involve assembly of the [2Fe-2S] cluster precursor on HydF by the endogenous iron–sulfur cluster machinery (ISC/SUF) of the cell (red pathways). Two pathways (colored black) rely on the delivery of an $Fe–(CO)_xCN$ species (see Figure 6) from HydG to HydF as precursor units of the full 2Fe subcluster. In either of these two pathways, either the HydF dimer (—) or the HydF tetramer (– – –) could interact with HydE and HydG. An additional possibility that is not depicted would involve formation of the decorated 2Fe subcluster on the HydF dimer from a standard [2Fe-2S] cluster, in a pathway that does not involve tetramer formation prior to the interaction with HydE and HydG. Gray arrows indicate the overlap of two or more pathways. The number of clusters per subunit is unknown, and we are presenting only one possibility associated with the interface between subunits within a single dimer. Color scheme: Fe, rust; S, yellow; C, gray; N, blue; O, red; unknown, magenta (see the legend of Figure 5); HydF dimer, green or light green.

**HydF Amino Acid Substitution Studies.** HydF contains several putative FeS cluster binding ligands in its C-terminal region, including Cys304, His306, His352, Cys353, and Cys356 (*Ca* numbering) (Figure 7). Substitutions of either Cys304 or Cys356 had significant effects on FeS cluster integrity, whereas substitutions of either Cys353 or His306 resulted in only moderately deleterious effects on FeS cluster binding.[59] HYSCORE spectroscopy has suggested the coordination of nitrogen to the [4Fe-4S] cluster of wild-type *Ca* HydF,[57] and site-directed mutagenic studies have provided additional insight into FeS cluster ligation environments. Costantini and co-


dx.doi.org/10.1021/bi500210x | *Biochemistry* 2014, 53, 4090–4104

workers have examined variants having either His306 or His352 substituted with Ala using both EPR and HYSCORE spectroscopic techniques and provided evidence that His352 is the fourth ligand to the [4Fe-4S] cluster in the *Ca* protein (Figure 5).[61] When HydF was expressed together with HydE and HydG, all substitutions except those at position His306 yielded HydF protein that was unable to activate $HydA^{\Delta EFG}$, although the His306 variants exhibited significantly reduced activity.[59] Further work with amino acid-substituted variants of *Tn* HydF is in line with the results summarized above for *Ca* HydF, namely, that the three Cys residues are required for [4Fe-4S] cluster coordination.[61,62] The structural, biochemical, and spectroscopic data together suggest a model in which FeS cluster coordination occurs at the dimer interface. Interestingly, no evidence of His-based nitrogen coordination was obtained in the HYSCORE spectra of either *Tm*[55,69] or *Tn* HydF,[61] and recent characterization of *Tn* HydF suggests that solvent-derived oxygen may be a ligand, leading to the conclusion that the fourth coordination site might be occupied by a labile or exchangeable ligand.[62] Further, results with *Tm* HydF show that both exogenous imidazole and His from the protein affinity tag can coordinate the [4Fe-4S] cluster in this enzyme, in line with the overall plasticity of cluster coordination.[69] Although significant effects on cluster coordination were not observed with substitution of His306 or His352, these residues were shown to be important for activation of $HydA^{\Delta EFG}$, and it is possible that these residues may stabilize the 2Fe subcluster species through hydrogen bonding interactions.

**GTPase Functionality and Maturase Interactions.** Initial annotation of the amino acid sequences of HydF revealed the presence of a canonical Walker A nucleotide binding motif, and GTP hydrolysis activity was subsequently shown.[55,56] The importance of HydF GTPase activity in hydrogenase maturation was demonstrated through site-directed mutagenic studies: HydF variants in which conserved *Ca* Walker P-loop motif residues Gly19, Gly24, and Ser26 were substituted with Ala were shown to be incapable of supporting the heterologous expression of active [FeFe]-hydrogenase in *E. coli* (Figure 2D).[39]

HydF GTP hydrolysis rates vary by as much as 40-fold in the presence of different monovalent cations, thus identifying HydF as belonging to a subclass of GTPase enzymes in which the alkali metal ion replaces the function of the "Arg finger" of GTPase activating proteins.[56] Additionally, both metal free and chemically reconstituted forms of *Ca* HydF displayed similar $k_{cat}$ values for GTP hydrolysis, relative to that of the as-purified enzyme; this suggests that the GTPase active site and the FeS cluster site(s) are distinct from one another.[56,68]

Interestingly, GTP was neither required nor provided stimulation for *in vitro* activation of $HydA^{\Delta EFG}$ by $HydF^{EG}$, indicating that GTP binding is not required for the 2Fe subcluster transfer and insertion step of maturation.[56] Because GTP binding or hydrolysis was not directly linked to the transfer of the 2Fe subcluster to $HydA^{\Delta EFG}$, it was hypothesized that it may be involved in prior steps during maturation involving HydE and/or HydG.[56] Assays in which HydF was incubated in the presence of either HydE or HydG revealed that GTP hydrolysis rates were stimulated by ~1.5-fold relative to that with HydF alone.[56] Additional evidence of protein−protein interactions between HydF and HydE and HydG has been reported in purification trials of the maturase proteins from coexpression cell lines.[53] In addition, surface plasmon resonance studies indicate that HydE binds to HydF with a $K_D$ ($9.19 \times 10^{-8}$ M), which is an order of magnitude lower than that for binding of HydG to HydF ($1.31 \times 10^{-6}$ M).[70] Competition experiments indicate that HydF can interact with only a single radical SAM enzyme at a time (Figure 6), and interactions appear to occur in a manner independent of the GTPase functionality, although doping GTP over either HydE−HydF or HydG−HydF complexes resulted in increased dissociation rates.[70]

## RADICAL SAM CHEMISTRY AND DIATOMIC LIGAND SYNTHESIS

**Tyrosine as the Source of Carbon Monoxide and Cyanide.** Among the members of the radical SAM enzyme superfamily, HydG is most closely related to ThiH, which catalyzes the degradation of Tyr into *p*-cresol and dehydroglycine (DHG), the latter of which is utilized during thiamine biosynthesis.[71−73] In addition to the radical SAM $CX_3CX_2C$ motif located in the N-terminal domain that is conserved in ThiH, HydG contains an accessory $CX_2CX_{22}C$ motif within an ~90-amino acid C-terminal domain (Figure 9).[38] Importantly,

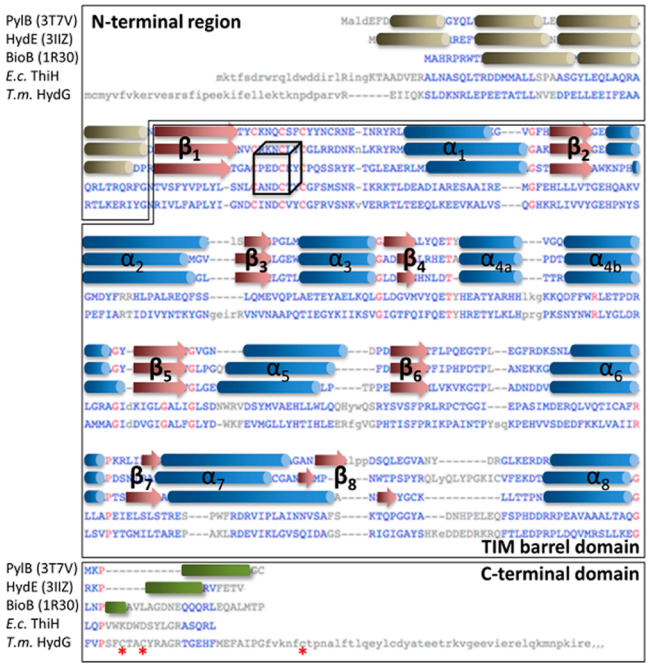


**Figure 9.** Sequence- and structure-based alignment of radical SAM enzymes with $(\beta\alpha)_8$ TIM barrels. Residues colored red are strictly conserved. Cylinders represent $\alpha$-helices (blue within the TIM barrel and brown outside). Red arrows are $\beta$-strands of the TIM barrel. The location of the canonical $CX_3CX_2C$ motif is signified by a cube. Green bars within boxed C-terminal regions represent residues that may cover the bottom of the barrel. Red asterisks denote cysteine residues that bind the C-terminal [4Fe-4S] cluster.

Cys to Ser substitutions in both the radical SAM and C-terminal domain motifs of HydG had significant impacts on the heterologous expression of active [FeFe]-hydrogenase in *E. coli* (Figure 2D).[39]

Given the close relationship between HydG and ThiH, Tyr was screened as a potential substrate for HydG and shown to increase rates of SAM cleavage and produce *p*-cresol as a reaction product.[74] Additionally, exogenously added Tyr was shown to enhance *in vitro* $HydA^{\Delta EFG}$ maturation, whereas no stimulation was observed with other Tyr analogues that lacked


dx.doi.org/10.1021/bi500210x | *Biochemistry* 2014, 53, 4090−4104

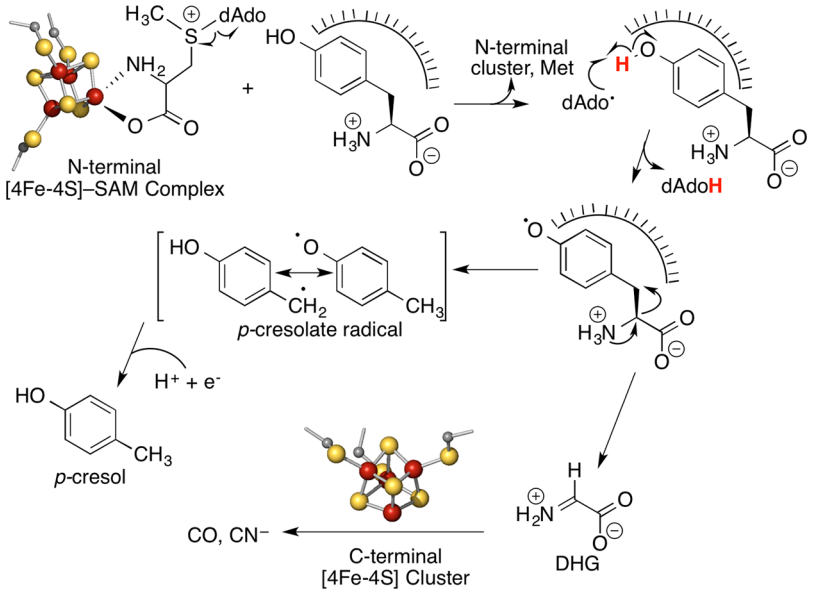


**Figure 10.** Hypothetical scheme detailing HydG's tyrosine lyase activity in the production of the diatomic ligands. Tyrosine is proposed to bind near the SAM-bound N-terminal [4Fe-4S] cluster. Following the reductive cleavage of SAM and the generation of dAdo•, the initial events of heterolytic tyrosine cleavage, including formation of the *p*-cresolate radical, presumably occur within the core TIM barrel structure. The product dehydroglycine is then converted into CO and $CN^-$ by components of the C-terminal domain and/or accessory FeS cluster. Although the mechanism of decomposition of dehydroglycine into CO and $CN^-$ is currently unresolved, it may occur through direct coordination to the C-terminal FeS cluster prior to breaking down into a [4Fe-4S]−cyano/carbonyl complex; this possibility is in line with results that provide evidence of coordination of a tyrosine-derived fragment to the C-terminal [4Fe-4S] cluster.[83,88] Color scheme: Fe, rust; S, yellow.

a *p*-hydroxyl group.[75] Collectively, the results support a mechanism in which HydG catalyzes the reductive cleavage of SAM to generate the 5′-deoxyadenosyl radical, which then abstracts an H atom from the phenolic position of tyrosine, in a manner similar to that proposed to occur in ThiH (Figure 10).[76,77] Such a mechanism readily accounts for the formation of *p*-cresol, but the inability to detect other HydG-based reaction products led to the proposal that HydG might be involved in the production of the dithiomethylamine ligand.[74]

Ultimately, turnover experiments performed with chemically reconstituted HydG in the presence of tyrosine revealed the formation of cyanide, which was trapped as the fluorescent 1-cyanobenz[*f*]isoindole (CBI) adduct and quantified using liquid chromatography−mass spectrometry techniques.[78] The cyanide adduct was concomitantly generated along with 5′-deoxyadenosine and *p*-cresol in near 1:1:1 stoichiometric quantities; assays conducted with uniformly labeled [U-$^{13}$C,$^{15}$N]tyrosine gave rise to a CBI compound with a mass increase of 2 *m*/*z* units, signifying incorporation of the [$^{15}$N]amino and [$^{13}$C]-*α*-carbon groups of tyrosine. Subsequent turnover experiments performed with HydG and tyrosine in the presence of deoxyhemoglobin (deoxyHb; $\lambda_{max}$ = 430 nm) revealed the isosbestic formation of carboxyhemoglobin (HbCO; $\lambda_{max}$ = 419 nm) that initially occurred via burst phase kinetics.[79] Assays conducted in the presence of [U-$^{13}$C,$^{15}$N]tyrosine led to the detection of an FTIR vibrational feature at 1907 $cm^{-1}$ characteristic of Hb$^{13}$CO, thereby validating the HydG-catalyzed synthesis of CO from tyrosine. Rate constants for the generation of CBI ($k_{cat}$ = 20 × $10^{-4}$ $s^{-1}$ at 37 °C) and HbCO ($k_{cat}$ = 11.4 × $10^{-4}$ $s^{-1}$ at 30 °C) species were quite comparable and implied that the diatomics originated from the same intermediate molecule.[78,79]

The detection and quantification of the production of $CN^-$ and CO by HydG were important discoveries but still left unanswered questions regarding the catalytic mechanism. For example, the amount of HbCO quantitated in assays is substoichiometric to the levels of 5′-deoxyadenosine and *p*-cresol that are formed over the same time course.[79] In addition, the presence of three CO and two $CN^-$ groups in the H-cluster raises the possibility that the third equivalent of CO could potentially be derived from an alternative substrate because the degradation of Tyr would yield *p*-cresol, CO, and $CN^-$ in expected 1:1:1 ratios (Figure 10). However, these issues were resolved in a series of HydA$^{\Delta EFG}$ maturation experiments using stable isotopically labeled Tyr species, confirming that all five H-cluster diatomic ligands are derived from tyrosine.[67]

**Iron−Sulfur Cluster States and Diatomic Ligand Biosynthesis.** As mentioned in the previous sections, both FeS cluster motifs present in the HydG sequence are critical for active [FeFe]-hydrogenase expression,[39] and formation of $CN^-$ and CO *in vitro* required the chemical reconstitution of as-purified HydG with $Fe^{2+}$ and $S^{2-}$.[78,79] Temperature-dependent EPR analysis of the photoreduced, as-purified *Ca* HydG showed both fast and slow relaxing signals, and these were attributed to a mixture of $[4Fe\text{-}4S]^+$ and $[2Fe\text{-}2S]^+$ clusters.[79] The chemically reconstituted form of HydG, on the other hand, clearly contained only fast relaxing $[4Fe\text{-}4S]^+$ cluster signals.[79] On the basis of the presence of both N- and C-terminal three-cysteine motifs in HydG, the spectroscopic data suggested that HydG coordinated two site-differentiated [4Fe-4S] clusters in its active form. Spectral simulations substantiated this proposal by showing that two distinct axial signals were present in the photoreduced enzyme state when SAM was present; it was proposed that SAM bound the N-terminal radical SAM cluster, but not the C-terminal cluster.[79]

Fontecilla-Camps and co-workers were the first to explore the role of the C-terminal [4Fe-4S] cluster via site-directed mutagenesis studies.[80,81] In their initial work, Nicolet et al. produced two variant *Ca* HydG proteins, one in which C-terminal cluster ligands Cys386 and Cys389 were substituted


dx.doi.org/10.1021/bi500210x | *Biochemistry* 2014, 53, 4090−4104

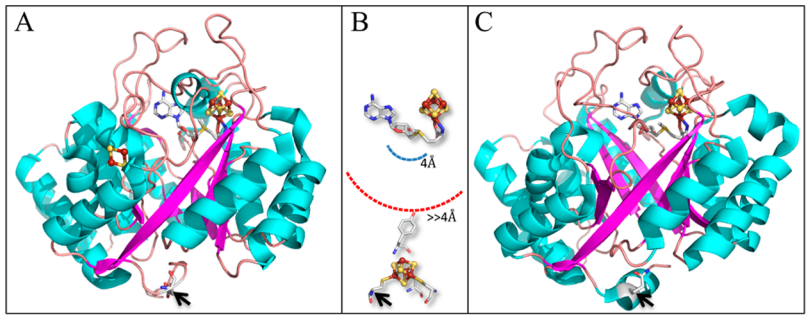


**Figure 11.** HydG structure-based template. (A) *Tm* HydE (PDB entry 3IIZ). (B) HydG cluster locations based on a homology model with respect to HydE and PylB crystal structures. The black arrows point to the location of the C*α* residues homologous to Cys386 (*Ca* numbering) in the $CX_2CX_{22}C$ cluster binding motif in the C-terminal domain of HydG. Tyrosine is modeled to scale at the hypothesized location at the C-terminal cluster. This presumably places the phenolic oxygen at a distance greater (red dashed line) than the average (blue dashed line) for H atom abstraction events within radical SAM enzymes (4.0 ± 0.4 Å). (C) *Mb* PylB (PDB entry 3T7V).

with Ser and the other in which the entire C-terminal FeS cluster binding domain was deleted (ΔCTD).[80] The Cys386- and Cys389-substituted HydG did not generate any CO but was able to produce significant amounts of $CN^-$, yielding ∼50% of the amount measured in the native enzyme. HydG ΔCTD did not produce any measurable CO or $CN^-$ but did demonstrate low levels of tyrosine lyase activity (2% of that of the wild type enzyme).[80,81]

We have recently provided new insights into the roles of the two [4Fe-4S] clusters in *Ca* HydG in a comparative study in which the spectroscopic and kinetic properties of C-terminal variants were analyzed together with variants that had substitutions in the N-terminal or radical SAM cluster ligands.[82] EPR spectroscopy demonstrated the presence of $[4Fe\text{-}4S]^+$ clusters in both the ΔCTD and radical SAM cluster variants upon photoreduction. Simulations of the EPR signatures for these two variants indicated these clusters displayed *g* values similar to what was observed in native HydG.[79] Moreover, no signal perturbations were observed with the addition of SAM to the radical SAM cluster variant, whereas addition of SAM to the ΔCTD variant results in a mixture of SAM-bound (73% of signal contributions) and unbound cluster states. These results suggest the C-terminal cluster cannot substitute for the N-terminal cluster with regard to SAM binding even though both clusters are site-differentiated. Collectively, the data allowed us to confidently assign *g* values for the N-terminal cluster in both SAM-bound and unbound states, as well as the C-terminal cluster, and these *g* value designations were used to accurately simulate the spectral signals of native HydG in the absence and presence of SAM.[82]

Recently, EPR spectral characterization of native *So* HydG revealed the presence of both $S = {}^1/_2$ $[4Fe\text{-}4S]^+$ signals in the $g \sim 2$ region along with low-field signals, with the latter interpreted as arising from a high-spin FeS cluster (possibly linear $[3Fe\text{-}4S]^+$ in nature) residing in the C-terminal accessory site. In this work, it was reported that addition of tyrosine to the reduced enzyme resulted in a large decrease in the signal intensity of the high-spin FeS cluster that was concomitant with the appearance of a small signal in the $g \sim 2$ region.[83] The large decrease in signal intensity was suggested to occur as a result of tyrosine-initiated cannibalization, resulting in the formation of the C-terminal $[4Fe\text{-}4S]^+$ cluster to which tyrosine was proposed to coordinate in N/O bidentate fashion.[83] We have not observed similar results in our work, and we do not see any evidence of the coordination of tyrosine to the accessory cluster in HydG in experiments performed on native and N-terminal variant HydG proteins. In both cases, only very subtle spectral perturbations were observed in the presence of tyrosine, indicating that either tyrosine does not coordinate the C-terminal cluster or its coordination does not result in the significant alteration of *g* values.[82] Previous spectroscopic studies of ThiH prepared in the presence of tyrosine either with or without SAM also do not show significant perturbations in FeS cluster EPR spectra.[84]

To gain further insight into tyrosine binding, we measured $K_{M\ Tyr}$ values for the native protein, a cysteine to serine variant (Cys386Ser), and ΔCTD HydG; $K_{M\ Tyr}$ values increased from 0.3 mM in the native enzyme to 1.6 mM in Cys386Ser to 10.6 mM in ΔCTD, while $K_{M\ SAM}$ values were roughly equivalent among these three forms.[82] Importantly, similar *p*-cresol formation rates for ΔCTD ($3.0 \times 10^{-3}$ $s^{-1}$), Cys386Ser ($4.3 \times 10^{-3}$ $s^{-1}$), and native ($4.4 \times 10^{-3}$ $s^{-1}$) enzymes coupled with substantial amounts of *p*-cresol formation (representing multiple turnover events within a 60 min assay period) were observed in assays. Thus, despite an apparent loss of binding affinity, these results indicate that catalytic steps can be rescued at higher substrate concentrations and the rates of radical formation and tyrosine cleavage are largely unaffected by mild to extreme alterations to the C-terminal domain and to its FeS cluster binding residues.[82] The effects on $K_{M\ Tyr}$, however, demonstrate that the C-terminal domain and its associated cluster provide important (though not essential) binding determinants for the substrate tyrosine.

While the HydG tyrosine lyase activity that yields *p*-cresol appears to occur within the TIM barrel, as previously suggested by Fontecilla-Camps and co-workers,[74,81] our results and those of others indicate that the accessory C-terminal domain and its FeS cluster play a critical role in formation of the diatomic ligands.[80,82,83] Our expanded characterization of variant HydG proteins has shown that Cys386Ser HydG generates 2.8 molar equiv of $CN^-$ and 0 equiv of CO, while ΔCTD HydG does not generate measurable equivalents of either CO or $CN^-$,[82] results that are in line with those of Nicolet et al.[80] Importantly, the decrease in $CN^-$:*p*-cresol ratios for ΔCTD and Cys386Ser in our work could be fully ascribed to stimulated glyoxylate levels.[78,82] Glyoxylate formation occurs through hydrolysis of DHG, the latter of which is hydrolytically unstable under *in vitro* assay conditions and is observed to form in equal amounts with *p*-cresol in the ThiH system.[73] The fact that glyoxylate is produced in the cases of Cys386Ser and ΔCTD HydG proteins points toward a heterolytic C*α*−C*β* bond cleavage mechanism


dx.doi.org/10.1021/bi500210x | *Biochemistry* 2014, 53, 4090−4104

for tyrosine, with the subsequent formation of dehydroglycine (Figure 10).

Confirmation of the heterolytic cleavage mechanism has been provided by rapid freeze-quench EPR experiments designed to trap intermediates during catalysis.[83] Turnover samples showed production of an FeS-based feature, as well as a transient $g = 2$ radical signal that disappeared with longer reaction times. HYSCORE and ENDOR spectral analysis of assays performed with uniformly labeled [$^{13}$C,$^{15}$N]tyrosine revealed evidence of both $^{15}$N and $^{13}$C coupling interactions with the FeS-based feature, indicating that either tyrosine or a tyrosine-derived species coordinates the C-terminal cluster.[83] The identity of the $g = 2$ radical was probed using various tyrosine isotopologs, and the pattern of hyperfine couplings was found to be consistent with a *p*-cresolate radical that would form upon heterolytic C$\alpha$−C$\beta$ tyrosine bond cleavage.

While the observations made from the spectroscopic and kinetic studies of HydG described above clearly provide evidence of the involvement of both [4Fe-4S] clusters in catalysis, with each cluster serving discrete roles in the mechanism, we propose that tyrosine does not bind to the C-terminal cluster of HydG as part of its mechanism. This line of reasoning originates from the body of knowledge of substrate location relative to SAM binding in other radical SAM enzymes, and the biochemical evidence that we have from studies of ThiH (Figure 11).[73,77,84] Sequence alignments of *Tm* HydG with *Tm* HydE, *Methanosarcina barkeri* (*Mb*) PylB, and *E. coli* BioB show that all four enzymes have complete $(\beta\alpha)_8$ TIM barrels (Figure 9).[85] The alignment also reveals that the $CX_2CX_{22}C$-containing domain of HydG begins immediately after the last $\alpha$-helix, as part of the environment covering the bottom lateral opening of the core TIM barrel structure. This suggests that the accessory [4Fe-4S] cluster bound to HydG caps the bottom of the TIM barrel where it is poised to bind a tyrosine-derived fragment.[74,81,85] The predicted HydG structure also supports this putative location for the C-terminal domain and cluster (Figure 11); the comparisons between the sequences of HydG and the known X-ray structures of HydE, PylB, and BioB indicate that the accessory [4Fe-4S] cluster would lie near the bottom of the TIM barrel roughly 26 Å from the N-terminal radical SAM cluster. This distance would appear to be too large to allow for abstraction of a H atom from tyrosine by the 5′-deoxyadenosyl radical generated at the radical SAM cluster (Figure 11). As a frame of reference, for known radical SAM structures in which SAM is cocrystallized along with either substrate or product molecules, distances between the 5′-C of SAM and the abstractable H atom fall within the range of 4.0 ± 0.4 Å.[85,86] For MoaA, an enzyme that utilizes an accessory [4Fe-4S] cluster to activate its GTP substrate, the distance between the site-differentiated iron ions of the two clusters is only 17.1 Å with GTP and SAM substrates bound directly between them (PDB entry 2FB3).[87]

Along these lines, we propose that tyrosine binds in the N-terminal domain, and upon heterolytic cleavage, the DHG moiety travels to the bottom of the barrel where subsequent reactions occur (Figures 10 and 11). Not only is this structural model consistent with that proposed previously,[81] but it fully acquiesces with the results that ΔCTD HydG catalytically resembles ThiH.[81,82] It is intriguing that in ThiH, one potential mechanism that has been put forth regarding the controlled synthesis of DHG from tyrosine, in a manner that precludes its hydrolysis to glyoxylate and ensures its incorporation into the thiazole carboxylate, includes it binding at the interface between ThiH and ThiG.[77] Along these lines, we propose that the fate of DHG in HydG is similarly controlled by the presence of the accessory domain and suggest that the $^{15}$N and $^{13}$C coupling interactions observed by Kuchenreuther et al. represent a fragment of tyrosine, possibly DHG, bound to the C-terminal cluster.[83]

Stopped-flow FTIR studies have provided some insight into the fate of DHG.[83,88] Experiments performed in the presence of myoglobin show that native *So* HydG forms both CO and $CN^-$ within 20 s of turnover initiation.[83] Similar assays performed with the Cys394Ser/Cys397Ser variant form of HydG showed only formation of $CN^-$ at longer time points, leading the authors to conclude that the $CN^-$ produced was not enzymatically relevant and that the accessory cluster is essential for the on-pathway formation of both diatomic species.[83] Additional work revealed the formation of two different Fe-bound diatomic complexes associated with the C-terminal cluster that develop under turnover conditions.[88] The first species is assigned as complex A and is composed of an Fe−CO/$CN^-$−[3Fe-4S] unit whose formation precedes that of complex B, presumably an $[Fe(II)(CO_2)CN)]^+$−[3Fe-4S] moiety.[88] The time-dependent decay of the *p*-cresolate radical occurs on a time scale similar to that of the formation of complex A, which is then converted to complex B following the consumption of a second molecule of tyrosine; the formation of complex B at this stage is proposed to occur concomitantly with the release of $CN^-$. Intriguingly, enzyme-derived CO was exogenously detected via binding to myoglobin only at longer time periods in these experiments, leading the authors to suggest that release of free CO by HydG is off-pathway,[88] a result that is in direct conflict with the rapid, burst phase production of CO in *Ca* HydG assays.[79] The fate of the HydG-derived $Fe(CO_2)CN$ unit has been traced by *in vitro* activation experiments performed with HydA, HydE, HydF, and $^{57}$Fe-loaded HydG; the resulting ENDOR spectrum for HydA demonstrates that the HydG-based organometallic product ultimately is incorporated into HydA as the 2Fe subcluster.[88]

The observation of the formation of Fe−diatomic species formed on HydG that are subsequently transferred to HydA[88] provides the impetus for revisiting aspects of our proposed overall mechanism of H-cluster biosynthesis and the specific role and function of HydF.[52,54] Clearly, the presence of the Fe−diatomic species on HydG that can be tracked to the functional hydrogenase precludes modification of Fe at a [2Fe-2S] site on HydF, as we have proposed.[56] However, in our work, we have yet to observe Fe−diatomic species on HydG and readily observe the production of free diatomic ligands in solution in native HydG activity assays, with the immediate, burst phase production of CO, suggesting that these do not initially bind to iron.[78,79,82] Moreover, the formation of Fe−diatomic species on HydG does not preclude a role for a [2Fe-2S] cluster bound to HydF, as it may act as a placeholder given the propensity the site must have to bind metal cluster intermediates, and biogenesis could proceed via replacement of Fe at this site (Figure 6). Given the range of observations from different research groups, and the ambiguity of the cluster composition and coordination of HydF in different states, it is premature to eliminate the possible functions and roles that have been proposed for HydF in H-cluster maturation (Figures 6 and 8).

There are differences observed in the characterization of both HydG and HydF that are at least intuitively contradictory. One experimental variable is the microbial sources of enzymes used by various research groups; however, there is no sound basis to

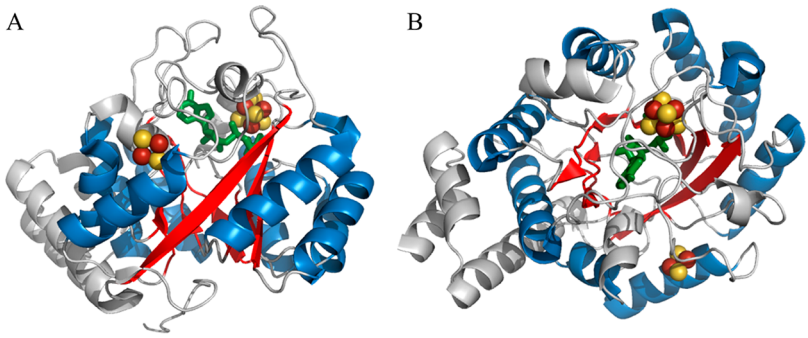


**Figure 12.** *Tm* HydE structure (PDB entry 3IIZ): (A) side view and (B) top view. Helices and strands in the TIM barrel are colored blue and red, respectively. SAM is colored green and shown in stick format.

anticipate that the mechanism of H-cluster biosynthesis would change as a function of microbial source. Experimental approaches also vary among the research groups working in the area; however, it is unclear how these assorted approaches would lead to the significantly different results observed. An imperative needs to be placed on resolving the reported differences, to improve our fundamental understanding of the complicated H-cluster assembly and [FeFe]-hydrogenase maturation process.

## HYDE AND THE SYNTHESIS OF THE DITHIOMETHYLAMINE LIGAND?

**An Unknown Substrate and Mechanism.** The demonstration that HydG synthesizes CO and $CN^-$, coupled with HydF's role as a scaffold/carrier protein, suggests that HydE functions in the synthesis of the bridging dithiomethylamine ligand (Figure 6).[52,54] As of the date of this writing, the HydE substrate and product still remain to be identified. Given that hydrogenase activation can readily be accomplished using *E. coli* cell free lysates in which *hydE*, *hydF*, and *hydG* from *Ca* are coexpressed (Figure 2), it is likely that HydE acts on a common metabolite.[22,39,47,75] It should be noted, however, that the observation of partial *in vitro* $HydA^{\Delta EFG}$ activation in the absence of HydE and HydF has been reported and interpreted to mean that HydE plays no part in the synthesis of the dithiomethylamine ligand (and that HydF may not scaffold 2Fe subcluster assembly).[60] The alternative hypothesis put forth by Swartz and co-workers instead involved the construction of an Fe−CO/$CN^-$ complex resembling the 2Fe subcluster within HydG that could also include the dithiomethylamine bridge formed via a tyrosine-derived fragment in a manner reminiscent of that initially proposed by Pilet et al.[60,74] Swartz and co-workers even invoked a yet unidentified protein in dithiomethylamine biosynthesis and relegated the role of HydE in H-cluster maturation to that of a chaperone protein, assisting in cluster translocation of the HydG cofactor among HydG, HydF, and $HydA^{\Delta EFG}$.[60] However, given the unique and sometimes difficult chemistries catalyzed by radical SAM enzymes,[35] as well as the early experimental work of King and Posewitz demonstrating all three Hyd accessory proteins play essential roles in hydrogenase maturation (Figure 2),[38,39] we strongly favor a hypothesis that invokes a critical role for HydE in H-cluster maturation related to dithiomethylamine production (Figure 6).

**HydE Structure and Iron−Sulfur Cluster States.** Preliminary biochemical characterization of chemically reconstituted *Tm* HydE showed that the enzyme could coordinate two $S = {}^1/_2$ $[4Fe\text{-}4S]^+$ clusters in the reduced state and could also nonproductively cleave SAM at a rate of 1 mol of deoxyadenosine per mole of HydE per hour.[41] For a number of years, HydE was frequently annotated as biotin synthase (BioB) because of the high degree of sequence similarity between these proteins and the presence of auxiliary FeS clusters.[89] Consequently, this led to proposals involving HydE's role in catalyzing a sulfur insertion reaction during 2Fe subcluster biosynthesis using an FeS cluster-derived sulfide akin to BioB-related chemistry,[42] yet unlike BioB, the radical SAM and auxiliary clusters of HydE (when the latter exist) are located on opposite sides of the TIM barrel at a distance of >21 Å.[89] This distance suggests that the sulfide ions of the accessory cluster are not utilized in a BioB-like insertion into the substrate.[90] Moreover, the cluster occupancy of this site is quite variable depending on protein preparation, and the cysteines used to bind the accessory cluster (Cys311, Cys319, and Cys322) are only partially conserved in known HydE sequences. Lastly, these cysteines can be successfully mutated without any deleterious effects on hydrogenase activation, suggesting that this cluster plays no essential role in the maturation process.[89]

Several crystal structures of HydE have been determined and show the complete $(\beta\alpha)_8$ TIM barrel fold of the enzyme (Figure 12).[89,91,92] Intriguingly, Nicolet et al. observed a high affinity of the enzyme for methionine and 5′-deoxyadenosine products and suggested that HydE may utilize SAM as a cofactor and not a cosubstrate.[91] The HydE structure revealed a large internal electropositive cavity spanning the full length of the TIM barrel that contained three distinct anion binding sites.[89] Thiocyanate bound with high affinity in the third site located at the bottom of the barrel. While it is still unknown why HydE would bind $SCN^-$ with such high affinity, the presence of such small anions could reflect a pathway by which the substrate reacts at the top of the barrel near the radical SAM cluster then the product migrates down to the bottom of the barrel for transfer to another protein.[89,93] Lastly, *in silico* docking studies suggested that the putative substrate binding pocket could accommodate a small molecule containing a carboxylate group and a partial positive charge. Despite the extensive structural work done with HydE, no real insight into its role in hydrogenase maturation has been revealed.

While HydE was originally reported to have a structure significantly similar to that of BioB,[89] suggesting synthesis of the dithiolate ligand by radical SAM catalyzed sulfur insertion into an alkyl substrate, more recent sequence and structure analysis has shown that HydE shares a greater resemblance to methylornithine synthase (PylB) (Figure 11A,C).[94] PylB is a radical SAM enzyme composed of a full $(\beta\alpha)_8$ TIM barrel that catalyzes the isomerization of L-lysine to L-methylornithine in


dx.doi.org/10.1021/bi500210x | *Biochemistry* 2014, 53, 4090−4104

the biosynthetic pathway of pyrrolysine, the 22nd naturally encoded amino acid.[94] DALI (distance alignment matrix method) analysis revealed that among all X-ray crystal structures, PylB was most similar to HydE and BioB, being 29.0 and 20.6% similar, respectively. Moreover, when PylB was superimposed with these structures, an rmsd of 1.3 Å was obtained with HydE, relative to an rmsd value of 1.8 Å with BioB. The overlay of the HydE and PylB crystal structures (PylB, PDB entry 3T7V; HydE, PDB entry 3CIW) shows comparable SAM and putative substrate binding pockets, potentially pointing to mechanistic similarities for these enzymes.[94] HydE has a much higher binding affinity for HydF than HydG does, and the two radical SAM proteins do not appear to interact with one another.[70] These data speak to the tightly controlled process that appears to exist during 2Fe subcluster biosynthesis and suggest that HydE may catalyze the first step in this reaction, delivering its product to HydF.[42,54] Further support for this hypothesis comes from the observation that in nature HydE and HydF exist as a fused *hydEF* gene in certain organisms.[95]

## ■ CONCLUSIONS

While many details of the H-cluster biosynthetic scheme still remain to be elucidated, the findings made in recent years have been imperative in clarifying many aspects of the maturation pathway and in illuminating some of the outstanding experimental questions that will undoubtedly guide future research. Some prominent research frontiers for the immediate future include resolving issues related to HydG's mechanism for the breakdown of dehydroglycine into the diatomic ligands, identifying HydE's substrate and a mechanism for incorporating the dithiolate ligand into the 2Fe subcluster, and defining HydF's role in H-cluster biosynthesis, including the nature of its function as a scaffold or carrier as well as the role of GTP binding and hydrolysis. The biochemical characterization of the steps involved in [FeFe]-hydrogenase maturation, including the description of H-cluster intermediate species, will surely continue to uncover the mysteries of nature's most prolific hydrogen catalyst.

## ■ AUTHOR INFORMATION

### Corresponding Author

*E-mail: jbroderick@chemistry.montana.edu.

### Funding

Our work on hydrogenase maturase proteins is supported by U.S. Department of Energy Grant DE-FG02-10ER16194 (to J.B.B., J.W.P., and E.M.S.) and Air Force Office of Scientific Research Grant FA-9550-11-1-0218 (to J.W.P.).

### Notes

The authors declare no competing financial interest.

## ■ ACKNOWLEDGMENTS

We thank Rebecca Driesener and Peter Roach for the collaboration on the research reviewed herein.

## ■ ABBREVIATIONS

*Ca*, *C. acetobutylicum*; CBI, 1-cyanobenz[*f*]isoindole; ΔCTD, HydG mutant with a truncated C-terminal domain; *Cp*, *C. pasteurianum*; CpI, [FeFe]-hydrogenase I from *C. pasteurianum*; *Cr*, *Ch. reinhardtii*; DALI, distance alignment matrix method; dAdo$^{\bullet}$, 5′-deoxyadenosyl radical; deoxyHb, deoxyhemoglobin; DHG, dehydroglycine; ENDOR, electron nuclear double-resonance spectroscopy; EPR, electron paramagnetic resonance spectroscopy; FeS, iron−sulfur; FTIR, Fourier transform infrared spectroscopy; GTP, guanosine triphosphate; HbCO, carboxyhemoglobin; HydA, [FeFe]-hydrogenase; HydA$^{\Delta EFG}$, HydA expressed without HydE, HydF, and HydG maturases; HydA$^{EFG}$, HydA coexpressed with HydE, HydF, and HydG maturases; HydF$^{\Delta EG}$, maturase protein HydF expressed without HydE and HydG; HydF$^{EG}$, maturase protein HydF coexpressed with HydE and HydG; HYSCORE, hyperfine sublevel correlation spectroscopy; ISC, iron−sulfur cluster assembly machinery; Δ*iscR*, deletion of the ISC repressor gene; NRVS, nuclear resonance vibrational spectroscopy; PDB, Protein Data Bank; rmsd, root-mean-square deviation; SAM, *S*-adenosyl-L-methionine; *So*, *S. oneidensis*; SUF, sulfur mobilization assembly machinery; ThiH, tyrosine lyase involved in thiamine biosynthesis; TIM barrel, triosephosphateisomerase-like tertiary fold; *Tm*, *T. maritima*; *Tn*, *T. neopolitana*; *Tt*, *Thermoanaerobacter tengcongensis*; WT, wild type; XAS, X-ray absorption spectroscopy.

## ■ REFERENCES

(1) Fontecilla-Camps, J. C., Amara, P., Cavazza, C., Nicolet, Y., and Volbeda, A. (2009) Structure-function relationships of anaerobic gas-processing metalloenzymes. *Nature 460*, 814−822.

(2) Mulder, D. W., Shepard, E. M., Meuser, J. E., Joshi, N., King, P. W., Posewitz, M. C., Broderick, J. B., and Peters, J. W. (2011) Insights into [FeFe]-hydrogenase structure, mechanism, and maturation. *Structure 19*, 1038−1052.

(3) Peters, J. W. (1999) Structure and mechanism of iron-only hydrogenases. *Curr. Opin. Struct. Biol. 9*, 670−676.

(4) Vignais, P. M., and Billoud, B. (2007) Occurrence, classification, and biological function of hydrogenases: An overview. *Chem. Rev. 107*, 4206−4272.

(5) Boer, J. L., Mulrooney, S. B., and Hausinger, R. P. (2014) Nickel-dependent metalloenzymes. *Arch. Biochem. Biophys. 544*, 142−152.

(6) Volbeda, A., Charon, M. H., Piras, C., Hatchikian, E. C., Frey, M., and Fontecilla-Camps, J. C. (1995) Crystal structure of the nickel-iron hydrogenase from *Desulfovibrio gigas*. *Nature 373*, 580−587.

(7) Happe, R. P., Roseboom, W., Pierik, A. J., Albracht, S. P., and Bagley, K. A. (1997) Biological activation of hydrogen. *Nature 385*, 126.

(8) Pierik, A. J., Hulstein, M., Hagen, W. R., and Albracht, S. P. (1998) A low-spin iron with CN and CO as intrinsic ligands forms the core of the active site in [Fe]-hydrogenases. *Eur. J. Biochem. 258*, 572−578.

(9) Pierik, A. J., Roseboom, W., Happe, R. P., Bagley, K. A., and Albracht, S. P. (1999) Carbon monoxide and cyanide as intrinsic ligands to iron in the active site of [NiFe]-hydrogenases. NiFe(CN)$_2$CO, biology's way to activate $H_2$. *J. Biol. Chem. 274*, 3331−3337.

(10) Peters, J. W., Lanzilotta, W. N., Lemon, B. J., and Seefeldt, L. C. (1998) X-ray crystal structure of the Fe-only hydrogenase (CpI) from *Clostridium pasteurianum* to 1.8 angstrom resolution. *Science 282*, 1853−1858.

(11) Nicolet, Y., Piras, C., Legrand, P., Hatchikian, C. E., and Fontecilla-Camps, J. C. (1999) *Desulfovibrio desulfuricans* iron hydrogenase: The structure shows unusual coordination to an active site Fe binuclear center. *Structure 7*, 13−23.

(12) Nicolet, Y., de Lacey, A. L., Vernede, X., Fernandez, V. M., Hatchikian, E. C., and Fontecilla-Camps, J. C. (2001) Crystallographic and FTIR spectroscopic evidence of changes in Fe coordination upon reduction of the active site of the Fe-only hydrogenase from *Desulfovibrio desulfuricans*. *J. Am. Chem. Soc. 123*, 1596−1601.

(13) Pandey, A. S., Harris, T. V., Giles, L. J., Peters, J. W., and Szilagyi, R. K. (2008) Dithiomethylether as a ligand in the hydrogenase H-cluster. *J. Am. Chem. Soc. 130*, 4533−4540.

(14) Giles, L. J., Grigoropoulos, A., and Szilagyi, R. K. (2011) Electron and spin density topology of the H-cluster and its biomimetic complexes. *Eur. J. Inorg. Chem.*, 2677−2690.
(15) Ryde, U., Greco, C., and De Gioia, L. (2010) Quantum refinement of [FeFe] hydrogenase indicates a dithiomethylamine ligand. *J. Am. Chem. Soc. 132*, 4512−4513.
(16) Grigoropoulos, A., and Szilagyi, R. K. (2010) Evaluation of the biosynthetic pathways for the unique dithiolate ligand of the FeFe hydrogenase H-cluster. *J. Biol. Inorg. Chem. 15*, 1177−1182.
(17) Silakov, A., Wenk, B., Reijerse, E., and Lubitz, W. (2009) $^{14}$N HYSCORE investigation of the H-cluster of [FeFe] hydrogenase: Evidence for a nitrogen in the dithiol bridge. *Phys. Chem. Chem. Phys. 11*, 6592−6599.
(18) Erdem, O. F., Schwartz, L., Stein, M., Silakov, A., Kaur-Ghumaan, S., Huang, P., Ott, S., Reijerse, E. J., and Lubitz, W. (2011) A model of the [FeFe] hydrogenase active site with a biologically relevant azadithiolate bridge: A spectroscopic and theoretical investigation. *Angew. Chem., Int. Ed. 50*, 1439−1443.
(19) Berggren, G., Adamska, A., Lambertz, C., Simmons, T. R., Esselborn, J., Atta, M., Gambarelli, S., Mouesca, J. M., Reijerse, E., Lubitz, W., Happe, T., Artero, V., and Fontecave, M. (2013) Biomimetic assembly and activation of [FeFe]-hydrogenases. *Nature 499*, 66−69.
(20) Esselborn, J., Lambertz, C., Adamska-Venkatesh, A., Simmons, T., Berggren, G., Noth, J., Siebel, J., Hemschemeier, A., Artero, V., Reijerse, E., Fontecave, M., Lubitz, W., and Happe, T. (2013) Spontaneous activation of [FeFe]-hydrogenases by an inorganic [2Fe] active site mimic. *Nat. Chem. Biol. 9*, 607−609.
(21) Bock, A., King, P. W., Blokesch, M., and Posewitz, M. C. (2006) Maturation of hydrogenases. *Adv. Microb. Physiol. 51*, 1−71.
(22) McGlynn, S. E., Ruebush, S. S., Naumov, A., Nagy, L. E., Dubini, A., King, P. W., Broderick, J. B., Posewitz, M. C., and Peters, J. W. (2007) In vitro activation of [FeFe] hydrogenase: New insights into hydrogenase maturation. *J. Biol. Inorg. Chem. 12*, 443−447.
(23) Forzi, L., and Sawers, R. G. (2007) Maturation of [NiFe]-hydrogenases in *Escherichia coli*. *BioMetals 20*, 565−578.
(24) Thauer, R. K., Kaster, A. K., Goenrich, M., Schick, M., Hiromoto, T., and Shima, S. (2010) Hydrogenases from methanogenic archaea, nickel, a novel cofactor, and $H_2$ storage. *Annu. Rev. Biochem. 79*, 507−536.
(25) Balk, J., Pierik, A. J., Netz, D. J., Muhlenhoff, U., and Lill, R. (2004) The hydrogenase-like Nar1p is essential for maturation of cytosolic and nuclear iron-sulphur proteins. *EMBO J. 23*, 2105−2115.
(26) Friedrich, T., and Scheide, D. (2000) The respiratory complex I of bacteria, archaea and eukarya and its module common with membrane-bound multisubunit hydrogenases. *FEBS Lett. 479*, 1−5.
(27) Posewitz, M., Mulder, D., and Peters, J. W. (2008) New frontiers in hydrogenase structure and biosynthesis. *Curr. Chem. Biol. 2*, 178−199.
(28) Watanabe, S., Sasaki, D., Tominaga, T., and Miki, K. (2012) Structural basis of [NiFe] hydrogenase maturation by Hyp proteins. *Biol. Chem. 393*, 1089−1100.
(29) Rangarajan, E. S., Asinas, A., Proteau, A., Munger, C., Baardsnes, J., Iannuzzi, P., Matte, A., and Cygler, M. (2008) Structure of [NiFe] hydrogenase maturation protein HypE from *Escherichia coli* and its interaction with HypF. *J. Bacteriol. 190*, 1447−1458.
(30) Lenz, O., Zebger, I., Hamann, J., Hildebrandt, P., and Friedrich, B. (2007) Carbamoylphosphate serves as the source of $CN^-$, but not of the intrinsic CO in the active site of the regulatory [NiFe]-hydrogenase from *Ralstonia eutropha*. *FEBS Lett. 581*, 3322−3326.
(31) Shomura, Y., and Higuchi, Y. (2012) Structural basis for the reaction mechanism of S-carbamoylation of HypE by HypF in the maturation of [NiFe]-hydrogenases. *J. Biol. Chem. 287*, 28409−28419.
(32) Stripp, S. T., Soboh, B., Lindenstrauss, U., Braussemann, M., Herzberg, M., Nies, D. H., Sawers, R. G., and Heberle, J. (2013) HypD is the scaffold protein for Fe-$(CN)_2CO$ cofactor assembly in [NiFe]-hydrogenase maturation. *Biochemistry 52*, 3289−3296.
(33) Soboh, B., Stripp, S. T., Bielak, C., Lindenstrauss, U., Braussemann, M., Javaid, M., Hallensleben, M., Granich, C., Herzberg, M., Heberle, J., and Sawers, R. G. (2013) The [NiFe]-hydrogenase accessory chaperones HypC and HybG of *Escherichia coli* are iron- and carbon dioxide-binding proteins. *FEBS Lett. 587*, 2512−2516.
(34) Olson, J. W., Mehta, N. S., and Maier, R. J. (2001) Requirement of nickel metabolism proteins HypA and HypB for full activity of both hydrogenase and urease in *Helicobacter pylori*. *Mol. Microbiol. 39*, 176−182.
(35) Broderick, J. B., Duffus, B. R., Duschene, K. S., and Shepard, E. M. (2014) Radical S-Adenosylmethionine Enzymes. *Chem. Rev. 114*, 4229−4317.
(36) Voordouw, G., Hagen, W. R., Kruse-Wolters, K. M., van Berkel-Arts, A., and Veeger, C. (1987) Purification and characterization of *Desulfovibrio vulgaris* (Hildenborough) hydrogenase expressed in *Escherichia coli*. *Eur. J. Biochem. 162*, 31−36.
(37) Atta, M., and Meyer, J. (2000) Characterization of the gene encoding the [Fe]-hydrogenase from *Megasphaera elsdenii*. *Biochim. Biophys. Acta 1476*, 368−371.
(38) Posewitz, M. C., King, P. W., Smolinski, S. L., Zhang, L., Seibert, M., and Ghirardi, M. L. (2004) Discovery of two novel radical S-adenosylmethionine proteins required for the assembly of an active [Fe] hydrogenase. *J. Biol. Chem. 279*, 25711−25720.
(39) King, P. W., Posewitz, M. C., Ghirardi, M. L., and Seibert, M. (2006) Functional studies of [FeFe] hydrogenase maturation in an *Escherichia coli* biosynthetic system. *J. Bacteriol. 188*, 2163−2172.
(40) Sofia, H. J., Chen, G., Hetzler, B. G., Reyes-Spindola, J. F., and Miller, N. E. (2001) Radical SAM, a novel protein superfamily linking unresolved steps in familiar biosynthetic pathways with radical mechanisms: Functional characterization using new analysis and information visualization methods. *Nucleic Acids Res. 29*, 1097−1106.
(41) Rubach, J. K., Brazzolotto, X., Gaillard, J., and Fontecave, M. (2005) Biochemical characterization of the HydE and HydG iron-only hydrogenase maturation enzymes from *Thermatoga maritima*. *FEBS Lett. 579*, 5055−5060.
(42) Peters, J. W., Szilagyi, R. K., Naumov, A., and Douglas, T. (2006) A radical solution for the biosynthesis of the H-cluster of hydrogenase. *FEBS Lett. 580*, 363−367.
(43) Florin, L., Tsokoglou, A., and Happe, T. (2001) A novel type of iron hydrogenase in the green alga *Scenedesmus obliquus* is linked to the photosynthetic electron transport chain. *J. Biol. Chem. 276*, 6125−6132.
(44) Happe, T., and Kaminski, A. (2002) Differential regulation of the Fe-hydrogenase during anaerobic adaptation in the green alga *Chlamydomonas reinhardtii*. *Eur. J. Biochem. 269*, 1022−1032.
(45) Forestier, M., King, P., Zhang, L., Posewitz, M., Schwarzer, S., Happe, T., Ghirardi, M. L., and Seibert, M. (2003) Expression of two [Fe]-hydrogenases in *Chlamydomonas reinhardtii* under anaerobic conditions. *Eur. J. Biochem. 270*, 2750−2758.
(46) Kamp, C., Silakov, A., Winkler, M., Reijerse, E. J., Lubitz, W., and Happe, T. (2008) Isolation and first EPR characterization of the [FeFe]-hydrogenases from green algae. *Biochim. Biophys. Acta 1777*, 410−416.
(47) Mulder, D. W., Ortillo, D. O., Gardenghi, D. J., Naumov, A. V., Ruebush, S. S., Szilagyi, R. K., Huynh, B., Broderick, J. B., and Peters, J. W. (2009) Activation of HydA(ΔEFG) requires a preformed [4Fe-4S] cluster. *Biochemistry 48*, 6240−6248.
(48) Silakov, A., Kamp, C., Reijerse, E., Happe, T., and Lubitz, W. (2009) Spectroelectrochemical characterization of the active site of the [FeFe] hydrogenase HydA1 from *Chlamydomonas reinhardtii*. *Biochemistry 48*, 7780−7786.
(49) Stripp, S., Sanganas, O., Happe, T., and Haumann, M. (2009) The structure of the active site H-cluster of [FeFe] hydrogenase from the green alga *Chlamydomonas reinhardtii* studied by X-ray absorption spectroscopy. *Biochemistry 48*, 5042−5049.
(50) Mulder, D. W., Boyd, E. S., Sarma, R., Lange, R. K., Endrizzi, J. A., Broderick, J. B., and Peters, J. W. (2010) Stepwise [FeFe]-hydrogenase H-cluster assembly revealed in the structure of HydA(ΔEFG). *Nature 465*, 248−251.

(51) Kuchenreuther, J. M., Guo, Y., Wang, H., Myers, W. K., George, S. J., Boyke, C. A., Yoda, Y., Alp, E. E., Zhao, J., Britt, R. D., Swartz, J. R., and Cramer, S. P. (2013) Nuclear resonance vibrational spectroscopy and electron paramagnetic resonance spectroscopy of $^{57}$Fe-enriched [FeFe] hydrogenase indicate stepwise assembly of the H-cluster. *Biochemistry 52*, 818−826.
(52) Peters, J. W., and Broderick, J. B. (2012) Emerging paradigms for complex iron-sulfur cofactor assembly and insertion. *Annu. Rev. Biochem. 81*, 429−450.
(53) McGlynn, S. E., Shepard, E. M., Winslow, M. A., Naumov, A. V., Duschene, K. S., Posewitz, M. C., Broderick, W. E., Broderick, J. B., and Peters, J. W. (2008) HydF as a scaffold protein in [FeFe] hydrogenase H-cluster biosynthesis. *FEBS Lett. 582*, 2183−2187.
(54) Shepard, E. M., Boyd, E. S., Broderick, J. B., and Peters, J. W. (2011) Biosynthesis of complex iron-sulfur enzymes. *Curr. Opin. Chem. Biol. 15*, 319−327.
(55) Brazzolotto, X., Rubach, J. K., Gaillard, J., Gambarelli, S., Atta, M., and Fontecave, M. (2006) The [Fe-Fe]-hydrogenase maturation protein HydF from *Thermotoga maritima* is a GTPase with an iron-sulfur cluster. *J. Biol. Chem. 281*, 769−774.
(56) Shepard, E. M., McGlynn, S. E., Bueling, A. L., Grady-Smith, C. S., George, S. J., Winslow, M. A., Cramer, S. P., Peters, J. W., and Broderick, J. B. (2010) Synthesis of the 2Fe subcluster of the [FeFe]-hydrogenase H cluster on the HydF scaffold. *Proc. Natl. Acad. Sci. U.S.A. 107*, 10448−10453.
(57) Czech, I., Silakov, A., Lubitz, W., and Happe, T. (2010) The [FeFe]-hydrogenase maturase HydF from *Clostridium acetobutylicum* contains a CO and CN- ligated iron cofactor. *FEBS Lett. 584*, 638−642.
(58) Czech, I., Stripp, S., Sanganas, O., Leidel, N., Happe, T., and Haumann, M. (2011) The [FeFe]-hydrogenase maturation protein HydF contains a H-cluster like [4Fe4S]-2Fe site. *FEBS Lett. 585*, 225−230.
(59) Joshi, N., Shepard, E. M., Byer, A. S., Swanson, K. D., Broderick, J. B., and Peters, J. W. (2012) Iron-sulfur cluster coordination in the [FeFe]-hydrogenase H cluster biosynthetic factor HydF. *FEBS Lett. 586*, 3939−3943.
(60) Kuchenreuther, J. M., Britt, R. D., and Swartz, J. R. (2012) New insights into [FeFe] hydrogenase activation and maturase function. *PLoS One 7*, e45850.
(61) Berto, P., Di Valentin, M., Cendron, L., Vallese, F., Albertini, M., Salvadori, E., Giacometti, G. M., Carbonera, D., and Costantini, P. (2012) The [4Fe-4S]-cluster coordination of [FeFe]-hydrogenase maturation protein HydF as revealed by EPR and HYSCORE spectroscopies. *Biochim. Biophys. Acta 1817*, 2149−2157.
(62) Albertini, M., Vallese, F., Di Valentin, M., Berto, P., Giacometti, G. M., Costantini, P., and Carbonera, D. (2014) The proton iron-sulfur cluster environment of the [FeFe]-hydrogenase maturation protein HydF from *Thermotoga neapolitana*. *Int. J. Hydrogen Energy*, DOI: 10.1016/j.ijhydene.2013.12.164.
(63) Chen, Z., Lemon, B. J., Huang, S., Swartz, D. J., Peters, J. W., and Bagley, K. A. (2002) Infrared studies of the CO-inhibited form of the Fe-only hydrogenase from *Clostridium pasteurianum* I: Examination of its light sensitivity at cryogenic temperatures. *Biochemistry 41*, 2036−2043.
(64) Adamska, A., Silakov, A., Lambertz, C., Rudiger, O., Happe, T., Reijerse, E., and Lubitz, W. (2012) Identification and characterization of the "super-reduced" state of the H-cluster in [FeFe] hydrogenase: A new building block for the catalytic cycle? *Angew. Chem., Int. Ed. 51*, 11458−11462.
(65) Mulder, D. W., Ratzloff, M. W., Shepard, E. M., Byer, A. S., Noone, S. M., Peters, J. W., Broderick, J. B., and King, P. W. (2013) EPR and FTIR analysis of the mechanism of $H_2$ activation by [FeFe]-hydrogenase HydA1 from *Chlamydomonas reinhardtii*. *J. Am. Chem. Soc. 135*, 6921−6929.
(66) Lubitz, W., Ogata, H., Rudiger, O., and Reijerse, E. (2014) Hydrogenases. *Chem. Rev. 114*, 4081−4148.
(67) Kuchenreuther, J. M., George, S. J., Grady-Smith, C. S., Cramer, S. P., and Swartz, J. R. (2011) Cell-free H-cluster synthesis and [FeFe] hydrogenase activation: All five CO and CN ligands derive from tyrosine. *PLoS One 6*, e20346.
(68) Cendron, L., Berto, P., D'Adamo, S., Vallese, F., Govoni, C., Posewitz, M. C., Giacometti, G. M., Costantini, P., and Zanotti, G. (2011) Crystal structure of HydF scaffold protein provides insights into [FeFe]-hydrogenase maturation. *J. Biol. Chem. 286*, 43944−43950.
(69) Berggren, G., Garcia-Serres, R., Brazzolotto, X., Clemancey, M., Gambarelli, S., Atta, M., Latour, J. M., Hernandez, H. L., Subramanian, S., Johnson, M. K., and Fontecave, M. (2014) An EPR/HYSCORE, Mössbauer, and resonance Raman study of the hydrogenase maturation enzyme HydF: A model for N-coordination to [4Fe-4S] clusters. *J. Biol. Inorg. Chem. 19*, 75−84.
(70) Vallese, F., Berto, P., Ruzzene, M., Cendron, L., Sarno, S., De Rosa, E., Giacometti, G. M., and Costantini, P. (2012) Biochemical analysis of the interactions between the proteins involved in the [FeFe]-hydrogenase maturation process. *J. Biol. Chem. 287*, 36544−36555.
(71) Begley, T. P., Downs, D. M., Ealick, S. E., McLafferty, F. W., Van Loon, A. P., Taylor, S., Campobasso, N., Chiu, H. J., Kinsland, C., Reddick, J. J., and Xi, J. (1999) Thiamin biosynthesis in prokaryotes. *Arch. Microbiol. 171*, 293−300.
(72) Begley, T. P. (2006) Cofactor biosynthesis: An organic chemist's treasure trove. *Nat. Prod. Rep. 23*, 15−25.
(73) Kriek, M., Martins, F., Challand, M. R., Croft, A., and Roach, P. L. (2007) Thiamine biosynthesis in *Escherichia coli*: Identification of the intermediate and by-product derived from tyrosine. *Angew. Chem., Int. Ed. 46*, 9223−9226.
(74) Pilet, E., Nicolet, Y., Mathevon, C., Douki, T., Fontecilla-Camps, J. C., and Fontecave, M. (2009) The role of the maturase HydG in [FeFe]-hydrogenase active site synthesis and assembly. *FEBS Lett. 583*, 506−511.
(75) Kuchenreuther, J. M., Stapleton, J. A., and Swartz, J. R. (2009) Tyrosine, cysteine, and S-adenosyl methionine stimulate in vitro [FeFe] hydrogenase activation. *PLoS One 4*, e7565.
(76) Leonardi, R., and Roach, P. L. (2004) Thiamine biosynthesis in *Escherichia coli*: In vitro reconstitution of the thiazole synthase activity. *J. Biol. Chem. 279*, 17054−17062.
(77) Challand, M. R., Martins, F. T., and Roach, P. L. (2010) Catalytic activity of the anaerobic tyrosine lyase required for thiamine biosynthesis in *Escherichia coli*. *J. Biol. Chem. 285*, 5240−5248.
(78) Driesener, R. C., Challand, M. R., McGlynn, S. E., Shepard, E. M., Boyd, E. S., Broderick, J. B., Peters, J. W., and Roach, P. L. (2010) [FeFe]-hydrogenase cyanide ligands derived from S-adenosylmethionine-dependent cleavage of tyrosine. *Angew. Chem., Int. Ed. 49*, 1687−1690.
(79) Shepard, E. M., Duffus, B. R., George, S. J., McGlynn, S. E., Challand, M. R., Swanson, K. D., Roach, P. L., Cramer, S. P., Peters, J. W., and Broderick, J. B. (2010) [FeFe]-hydrogenase maturation: HydG-catalyzed synthesis of carbon monoxide. *J. Am. Chem. Soc. 132*, 9247−9249.
(80) Nicolet, Y., Martin, L., Tron, C., and Fontecilla-Camps, J. C. (2010) A glycyl free radical as the precursor in the synthesis of carbon monoxide and cyanide by the [FeFe]-hydrogenase maturase HydG. *FEBS Lett. 584*, 4197−4202.
(81) Tron, C., Cherrier, M. V., Amara, P., Martin, L., Fauth, F., Fraga, E., Correard, M., Fontecave, M., Nicolet, Y., and Fontecilla-Camps, J. C. (2011) Further Characterization of the [FeFe]-Hydrogenase Maturase HydG. *Eur. J. Inorg. Chem.*, 1121−1127.
(82) Driesener, R. C., Duffus, B. R., Shepard, E. M., Bruzas, I. R., Duschene, K. S., Coleman, N. J., Marrison, A. P., Salvadori, E., Kay, C. W., Peters, J. W., Broderick, J. B., and Roach, P. L. (2013) Biochemical and kinetic characterization of radical S-adenosyl-L-methionine enzyme HydG. *Biochemistry 52*, 8696−8707.
(83) Kuchenreuther, J. M., Myers, W. K., Stich, T. A., George, S. J., Nejatyjahromy, Y., Swartz, J. R., and Britt, R. D. (2013) A radical intermediate in tyrosine scission to the CO and $CN^-$ ligands of FeFe hydrogenase. *Science 342*, 472−475.

(84) Kriek, M., Martins, F., Leonardi, R., Fairhurst, S. A., Lowe, D. J., and Roach, P. L. (2007) Thiazole synthase from *Escherichia coli*: An investigation of the substrates and purified proteins required for activity in vitro. *J. Biol. Chem. 282*, 17413−17423.
(85) Betz, J. N., Shepard, E. M., and Broderick, J. B. (2014) Radical S-adenosylmethionine (SAM) enzymes and their roles in complex cluster assembly. In *Metalloproteins: New Insights from Theory and Experiment with Implications for Experiments and Challenges to the Theory* (Cho, A., and Goddard, W. A., Eds.) CRC Press, Boca Raton, FL (in press).
(86) Vey, J. L., and Drennan, C. L. (2011) Structural insights into radical generation by the radical SAM superfamily. *Chem. Rev. 111*, 2487−2506.
(87) Hanzelmann, P., and Schindelin, H. (2006) Binding of 5′-GTP to the C-terminal FeS cluster of the radical S-adenosylmethionine enzyme MoaA provides insights into its mechanism. *Proc. Natl. Acad. Sci. U.S.A. 103*, 6829−6834.
(88) Kuchenreuther, J. M., Myers, W. K., Suess, D. L., Stich, T. A., Pelmenschikov, V., Shiigi, S. A., Cramer, S. P., Swartz, J. R., Britt, R. D., and George, S. J. (2014) The HydG enzyme generates an $Fe(CO)_2(CN)$ synthon in assembly of the FeFe hydrogenase H-cluster. *Science 343*, 424−427.
(89) Nicolet, Y., Rubach, J. K., Posewitz, M. C., Amara, P., Mathevon, C., Atta, M., Fontecave, M., and Fontecilla-Camps, J. C. (2008) X-ray structure of the [FeFe]-hydrogenase maturase HydE from *Thermotoga maritima*. *J. Biol. Chem. 283*, 18861−18872.
(90) Fugate, C. J., and Jarrett, J. T. (2012) Biotin synthase: Insights into radical-mediated carbon-sulfur bond formation. *Biochim. Biophys. Acta 1824*, 1213−1222.
(91) Nicolet, Y., Amara, P., Mouesca, J. M., and Fontecilla-Camps, J. C. (2009) Unexpected electron transfer mechanism upon AdoMet cleavage in radical SAM proteins. *Proc. Natl. Acad. Sci. U.S.A. 106*, 14867−14871.
(92) Nicolet, Y., Rohac, R., Martin, L., and Fontecilla-Camps, J. C. (2013) X-ray snapshots of possible intermediates in the time course of synthesis and degradation of protein-bound $Fe_4S_4$ clusters. *Proc. Natl. Acad. Sci. U.S.A. 110*, 7188−7192.
(93) Nicolet, Y., and Fontecilla-Camps, J. C. (2012) Structure-function relationships in [FeFe]-hydrogenase active site maturation. *J. Biol. Chem. 287*, 13532−13540.
(94) Quitterer, F., List, A., Eisenreich, W., Bacher, A., and Groll, M. (2012) Crystal structure of methylornithine synthase (PylB): Insights into the pyrrolysine biosynthesis. *Angew. Chem., Int. Ed. 51*, 1339−1342.
(95) Duffus, B. R., Hamilton, T. L., Shepard, E. M., Boyd, E. S., Peters, J. W., and Broderick, J. B. (2012) Radical AdoMet enzymes in complex metal cluster biosynthesis. *Biochim. Biophys. Acta 1824*, 1254−1263.